JOURNAL OF SPACECRAFT AND ROCKETS
Vol. 45, No. 1, January–February 2008

Deep Impact Navigation System Performance

Raymond B. Frauenholz,* Ramachandra S. Bhat,† Steven R. Chesley,† Nickolaos Mastrodemos,‡
William M. Owen Jr.,§ and Mark S. Ryne‡
Jet Propulsion Laboratory, California Institute of Technology, Pasadena, California 91109

DOI: 10.2514/1.24310

Deep Impact successfully met its primary mission objective on 4 July 2005 when the smart impactor guided itself into the path of Comet 9P/Tempel 1. The mother flyby spacecraft then observed and recorded the breathtaking collision and subsequent plume development. Ground-based navigators targeted the prerelease trajectory using optical navigation image planning and data analysis, trajectory correction maneuver design and evaluation, and orbit determination using both radiometric and optical data. In-flight improvements to the Tempel 1 ephemeris were also a critical part of the overall navigation design and operations success. The achieved navigation accuracy established a new standard for comet encounters, and this difficult task taught several important lessons. This definitive work provides a mission overview, summarizes the navigation requirements, compares the achieved navigation performance with a baseline design that reflects in-flight updates, and identifies operational procedures that may benefit future comet-bound navigators.

Introduction

DEEP Impact, the eighth mission of NASA's Discovery Program, successfully met its primary objective on 4 July 2005 when the impactor spacecraft guided itself into the path of comet 9P/Tempel 1. The mother flyby spacecraft then observed and recorded the collision and subsequent plume formation. The two spacecraft were launched together as a single flight system on 12 January 2005 from Cape Canaveral, Florida, on a Boeing Delta II 7925 launch vehicle.

The major challenge for ground-based navigators was to place the flight system on the best achievable comet-intercept trajectory at impactor release so that the impactor could then autonomously guide itself to the desired impact location. In-flight improvements in the Tempel 1 ephemeris were a critical part of this ambitious objective. The Deep Space 1 encounter [1,2] with comet 19P/Borrelly in 2001 and the 2004 Stardust encounter [3–5] with comet 81P/Wild 2 used onboard cameras and optical navigation techniques to improve comet-relative trajectory accuracy for targets at flyby distances of several hundred kilometers. These recent encounters provided valuable experience needed to improve comet ephemeris and flight system navigation accuracies essential to meeting the demanding Deep Impact mission objectives. However, to achieve a near-intercept trajectory with the flight system followed by precision impactor targeting also required much improved knowledge of Tempel 1's physical properties such as its size, shape, topography, pole location and rotation period, and the relative brightness of the nucleus and coma. Our understanding of these physical characteristics was initially very limited, but steadily improved as the flight system neared Tempel 1. Very accurate flight system maneuver performance contributed significantly to the precise targeting of the prerelease intercept trajectory. These trajectory correction maneuvers (TCMs) were designed using orbit determination based on radiometric, interferometric, and onboard optical data, plus a very methodical comet ephemeris update process that made use of both ground-based and onboard astrometric measurements.

Multidisciplined ground-based navigation functions and onboard autonomous navigation systems and supporting flight software set a new accuracy standard for comet missions, and there were several important lessons learned in the process. These lessons often identified correctable problems to avoid in the future, but in several instances, good plans paid off and should also be remembered.

This paper summarizes the mission objectives and briefly describes the reference trajectory, the mission phases, and the spacecraft. The requirements placed on navigation are reviewed, including target delivery accuracies, TCM ΔV requirements and pointing-constraint compliance, and the go/no-go decision criteria for critical encounter events. The actual performance is compared with the navigation plan, noting important differences and the lessons learned. These assessments chronicle the performance of each navigation function: optical navigation analysis (referred to here as Opnav, whereas opnav refers to the data); maneuver design and evaluation; orbit determination (referred to as OD) using radiometric, interferometric, and optical data; comet ephemeris development; and onboard autonomous navigation (referred to as Autonav).

The flyby survived the Tempel 1 encounter in good health and was soon retargeted to an Earth flyby in late 2007 in preparation to support a new NASA Discovery Program mission called EPOXI, combining two diverse science objectives with a single spacecraft: Deep Impact Extended Investigation (DIXI) and Extrasolar Planet Observations and Characterization (EPOCh). A decision will be made by November 2007 whether EPOXI is targeted to observe comet 85P/Boethin during a close flyby in December 2008[¶] or is targeted for an encounter of comet 103P/Hartley 2 in December 2011. Because the flyby continues in good health, it is referred to here in the present tense, whereas the impactor is fondly referred to in the past tense.

Mission Overview

Mission Objectives

The Deep Impact mission team was led by its principal investigator, Michael A'Hearn of the University of Maryland. The

Presented as Paper 173 at the 16th AAS/AIAA Space Flight Mechanics Conference, Tampa, FL, 22–26 January 2006; received 8 February 2007; revision received 27 August 2007; accepted for publication 11 September 2007.

*Senior Member of Technical Staff, Deep Impact Navigation Team Chief, 4800 Oak Grove Drive.
†Senior Member of Technical Staff, 4800 Oak Grove Drive. Member AIAA.
‡Senior Member of Technical Staff, 4800 Oak Grove Drive.
§Principal Member of Technical Staff, 4800 Oak Grove Drive.

¶Efforts to acquire ground-based astrometry measurements to reduce the Boethin ephemeris uncertainty are ongoing (as this paper goes to press); targeting instead to Hartley 2 is not a currently approved option.

mission team included a science team of prominent experts on comets, remote sensing, and impact physics; the industrial partner Ball Aerospace & Technologies Corporation (BATC) that built the flight system; and the Jet Propulsion Laboratory that managed the project and conducted flight operations for NASA's Discovery Program.

In response to NASA's Announcement of Opportunity in 1999, Deep Impact was first proposed as an 18-month mission to be launched in December 2003. Blume [6] described this early mission design concept, and A'Hearn et al. [7] outlined the primary science objectives. The science objectives were very successfully met, except for viewing of the impact crater, due to an unexpectedly opaque and long-lasting dust plume,** but the encounter did reveal previously unknown physical properties of a comet. Early assessments suggest that Tempel 1 is held together more by gravity than by the cohesiveness of its materials. A'Hearn and his science team colleagues published their initial findings in a special issue of *Science* [8] dedicated to Deep Impact.

Reference Trajectory

The direct interplanetary trajectory depicted in Fig. 1 was designed to support launch between 30 December 2004 and 28 January 2005, with a Tempel 1 encounter on 4 July 2005. This encounter time was just one day before Tempel 1 perihelion passage at a heliocentric distance of 1.5 AU. The original project baseline was to launch a year earlier [6] and use the one-year Earth-to-Earth segment to link up with the 2005 direct-trajectory opportunity. The Earth flyby served only to advance the project launch schedule and was not required for mission performance. However, the earlier launch strategy did fit a shorter development schedule and provided more time to conduct in-flight payload and spacecraft tests, but the project encountered hardware delivery and testing delays that resulted in a one-year launch slip. Blume [9] described the mission design update for the direct trajectory.

The 4 July 2005 encounter time was nearly optimum because it allowed a near-maximum payload mass and a reasonable solar phase angle (sun–probe–comet angle), important to comet imaging during approach. Later arrival times allowed for modest increases in payload mass, but degraded the approach phase angle; earlier dates improved the phase angle, but with a significant falloff in mass capability. Earlier arrival dates would have increased the approach velocity (10.2 km/s) and in turn required a larger flyby divert maneuver or reduced the observing time achievable by the divert maneuver.

Mission Phases

The six-month mission was divided into distinct functional phases, as described by the overview in Fig. 2. Ground navigation actively supported each mission phase, including launch, all TCMs, the optical navigation (Opnav) campaign scheduled to begin near $E-60$ days, and a busy encounter timeline. The Opnav and Autonav activities depended on calibrations during commissioning and cruise to determine the orientation of each camera bore sight with respect to the flight system coordinate frame. Without these calibrations, camera-pointing errors could be interpreted as comet ephemeris errors during Autonav imaging,†† and this could result in navigation errors.

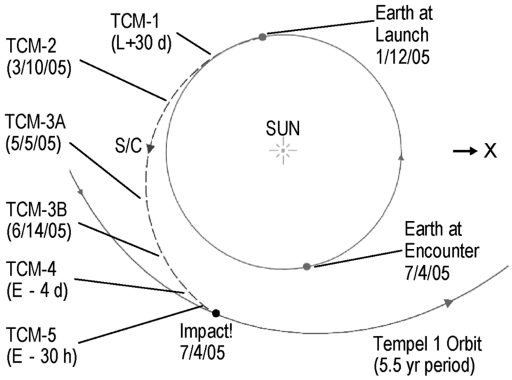

Fig. 1 Interplanetary reference trajectory.

Flight System

The primary element of the flight system depicted in Fig. 3a is the flyby spacecraft, designed to carry and target the impactor spacecraft for release as early as 24 h before impact. The flyby also provided a stable platform for remote sensing of the comet nucleus before, during, and after the impact event, and it provides the communications node for storage and return of scientific data to Earth.

The total flight system mass at launch was 973 kg. The total flyby portion was 601 kg, including a full tank of hydrazine monopropellant (85 kg of fuel and 0.6 kg of pressurant). Four 22-N thrusters are used to apply thrust along the $+X$ body axis for TCMs. The solar array mounted normal to the $+Y$ axis has an area of 7.9 m^2. The impactor total wet mass was 372 kg, including 7.8 kg of hydrazine propellant for impactor targeting maneuvers (ITMs) following release. The impactor mass included 113 kg of copper dead weight to increase the effectiveness of cratering on impact. Copper was chosen because it was not expected to be present in the nucleus and its spectral lines could be easily removed from observations.

The flight system attitude is three-axis stabilized using both momentum wheels and thrusters. The baseline cruise attitude, depicted in Fig. 3b, maintained the sun in the body X–Y plane with the solar array offset by an open-loop "tip" angle profile to keep the center of pressure (CP) in near-alignment with the center of mass (CM) to best minimize the rate of momentum growth. Because of thermal constraints on the flight system top deck, the tip angle could not be larger than 30 deg. As a result, this open-loop CPCM strategy could not by itself maintain momentum within the reaction wheels' functional limit (2 $Nm \cdot s$). Propulsive desaturation maneuvers (desats) using pairs of reaction control system (RCS) thrusters were periodically required, but preflight estimates indicated that only one desat per month would be necessary. These ground-commanded desats could use a coupled RCS thruster pair with nonzero (but small) net ΔV or an uncoupled RCS set, resulting in a net ΔV. The flight system ADCS could autonomously execute an uncoupled desat should momentum buildup reach a preset threshold, and this would introduce an unplanned ΔV in the flight system trajectory. During flight, the number of desats was considerably larger than once per month predicted by preflight estimates, and they were all uncoupled. The implications of this change to navigation operations will be discussed later in the paper.

For telecom, the flyby uses a steerable X-band high-gain antenna (HGA) that points to Earth via gimbal rotations about the Y and Z body axes. The HGA was the preferred antenna throughout the mission; at encounter it served to downlink valuable encounter data in real time at rates of up to 200 kbps (kilobits per second). Also available are single broad-beam low-gain antennas centered on the $+Y$ (LGA-1) and $-Y$ (LGA-2) axes. The choice of antenna ultimately depends on the flight attitude, Earth distance, the availability of either 34- or 70-m ground stations, and the desired data rate.

The flyby has two cameras, each used for both science observations and optical navigation. The high-resolution imager

**A NASA Discovery Program mission called Stardust-NExT (new exploration of Tempel 1) has been approved to retarget the Stardust spacecraft, which has completed its prime mission, to encounter Tempel 1 during its 2011 perihelion passage. NExT will expand the investigation of Tempel 1, including imaging the impact crater made by Deep Impact.

††Opnav used stars to determine pointing; the big risk was that bad values of the camera alignment would move stars or the comet out of the image subframe (1008 × 1008 pixels, see Table 1). Autonav did not directly use stars, but did rely on attitude determination and control system (ADCS) pointing information from star-trackers.

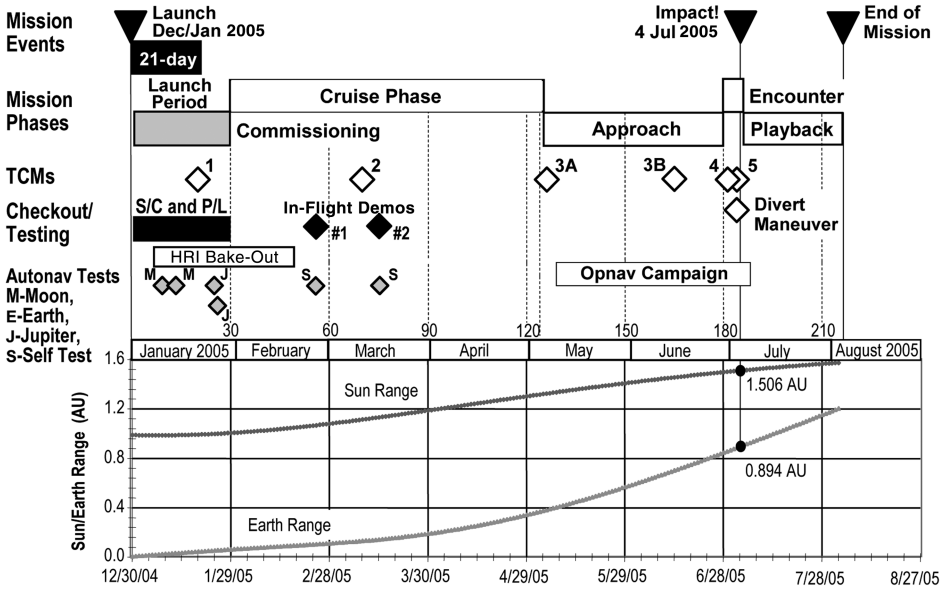

Fig. 2 Overview of the mission timeline.

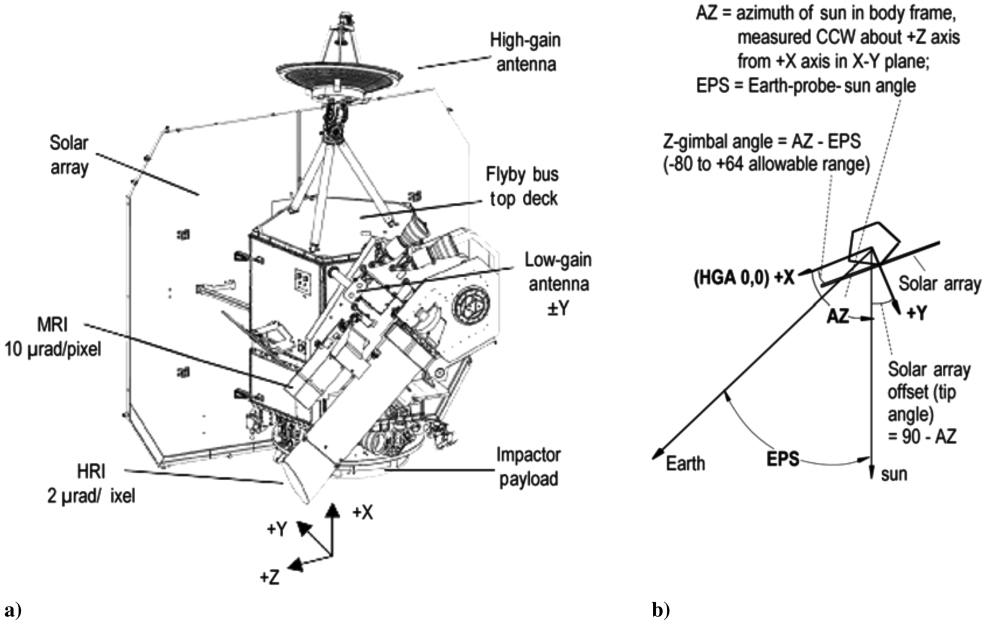

a) b)

Fig. 3 Flight system a) configuration and b) cruise attitude strategy.

(HRI) has a resolution of 2 μrad/pixel. The HRI feeds a 1024 × 1024 pixel charge-coupled device (CCD) through a filter wheel for visual observations and an imaging infrared spectrometer that covers wavelengths between 1.05 and 4.8 μm. The separate medium-resolution imager (MRI) has the same CCD and filter-wheel sensor design with a factor-of-five lower resolution of 10 μrad/pixel. Other key physical properties of these flyby cameras are summarized in Table 1. The impactor had a single camera, the impactor targeting sensor (ITS), with optical properties identical to the flyby's MRI but without the filter wheel.

Navigation Design

The navigation design addresses the target delivery accuracy requirements and the strategies needed to meet them. This design includes support from orbit determination, optical navigation, Tempel 1 ephemeris development, the TCM campaign with pointing-constraint compliance, and specific go/no-go decision criteria near encounter chosen to balance delivery accuracy requirements with operational considerations.

Target Delivery Accuracy Requirements

The primary requirements on ground-based navigation specified the flight system target delivery accuracy needed for impactor release and the flyby target delivery accuracy at Tempel 1 closest approach

Table 1 Camera properties

Parameter	HRI	MRI
Aperture, cm	30	12
CCD format, pixels	1024 × 1024	1024 × 1024
Pixel size, μm	21	21
Charge capacity, electrons	>450, 000	>450, 000
Focal length, m	10.5	2.1
Resolution, μrad/pixel	2	10
Field of view, deg	0.117	0.587
Focal ratio	$f/35$	$f/21$
Shutter speeds	10 ms–64 s	10 ms–20 s
Readout rate	1 full frame/1.8 s	1 full frame/1.8 s
Digitization	14 bits	14 bits
Saved images	1008 × 1008	1008 × 1008

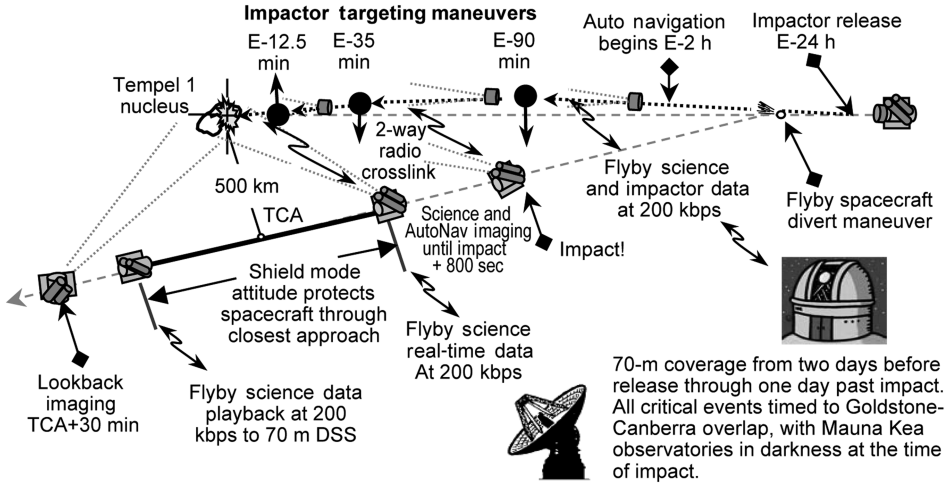

Fig. 4 Encounter schematic (view toward the sun, not to scale).

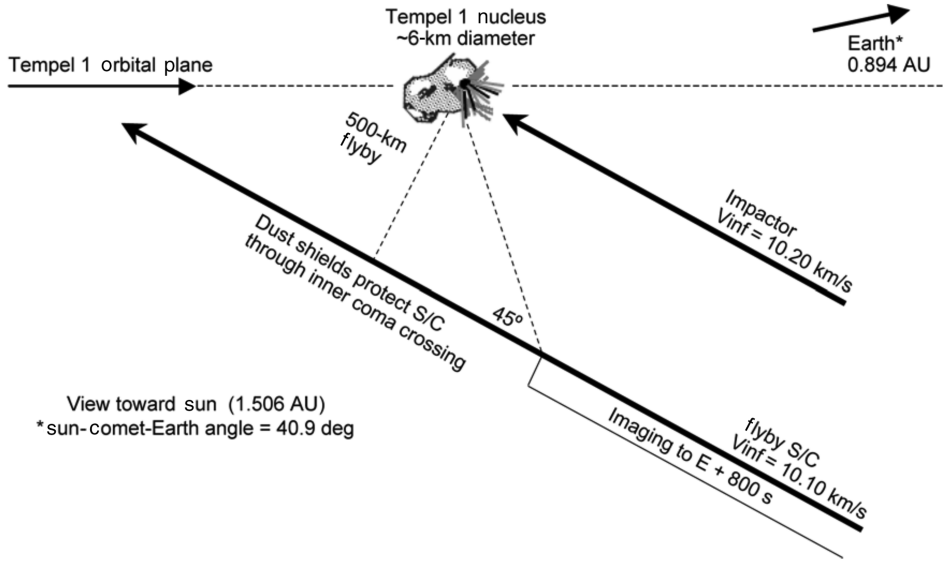

Fig. 5 Trajectory at Tempel 1 impact (view toward the sun, not to scale).

relative to *actual* impact. These events are depicted in the encounter schematic in Fig. 4. The flight system delivery for impactor release was to be within 30 km (3σ) of the estimated comet nucleus for release at E − 24 h. This requirement served to limit the impactor ΔV for ITM-1 at E − 90 min to 5 m/s, or about 20% of the total impactor maneuver capability. A flyby divert maneuver 12 min after impactor release was designed to achieve a 500-km flyby altitude and to delay the time of closest approach (TCA) by 850 s relative to the *actual* time of impact (TOI). That is, $(\mathrm{TCA}_{\mathrm{flyby}} - \mathrm{TOI}_{\mathrm{impactor}}) = 850$ s. This delay provided an observing time of 800 s after TOI before the flyby entered shield mode for protection from dust particles as it crossed through Tempel 1's inner coma (Fig. 5).

The achievable target delivery accuracy depended heavily on the comet physical properties, and we knew very little about Tempel 1. Among the most important cometary properties of concern to us were the nucleus topography and the dust environment (coma). The Deep Impact science team defined bounding physical models, referred to as *most likely coma* (MLC) and *worst likely coma* (WLC) models of the nucleus size, shape, and topographic relief for use in developing representative navigation strategies. We used these models to better understand the navigation sensitivities to nucleus makeup by comparing predicted delivery accuracies and the attendant nucleus impact probabilities.

The flyby B-plane[‡‡] aim point, shown in Fig. 6a, was selected to place the comet-centered radius vector $\boldsymbol{B}$ at closest approach normal to the sun direction, thus affording excellent viewing geometry of impact in a sunlit area. The divert maneuver introduced a predetermined change from the finally targeted prerelease trajectory and, as such, was deterministic. Because the flyby and impactor shared the same comet-relative trajectory errors at release, the flyby delivery errors were expected to be dominated by the divert execution errors. The specified 3σ divert control requirements were ±50 km in the 500-km B-plane target and ±20 s in the 850-s delay time. Figure 6b shows the wedge-shaped region acceptable for the B-plane parameters achieved by the divert maneuver. The lower altitude limit satisfied our concerns about the hazards of the dust environment, and the upper bound limited loss of imaging resolution. The angular dimensions of the wedge, equivalent to ±50 km at 500-km altitude, provided an attitude control authority margin necessary to maintain planned camera-pointing during the flyby.

[‡‡]The target B plane contains the comet and the flyby miss vector $\boldsymbol{B}$ and is normal to the flight system incoming inertial velocity direction S. The B-plane T axis is normal to S and parallel to the Earth mean equator and equinox of 2000 (EME2000); the R axis $= S \times T$. The $\boldsymbol{B}$ vector has components $B \cdot R$ and $B \cdot T$.

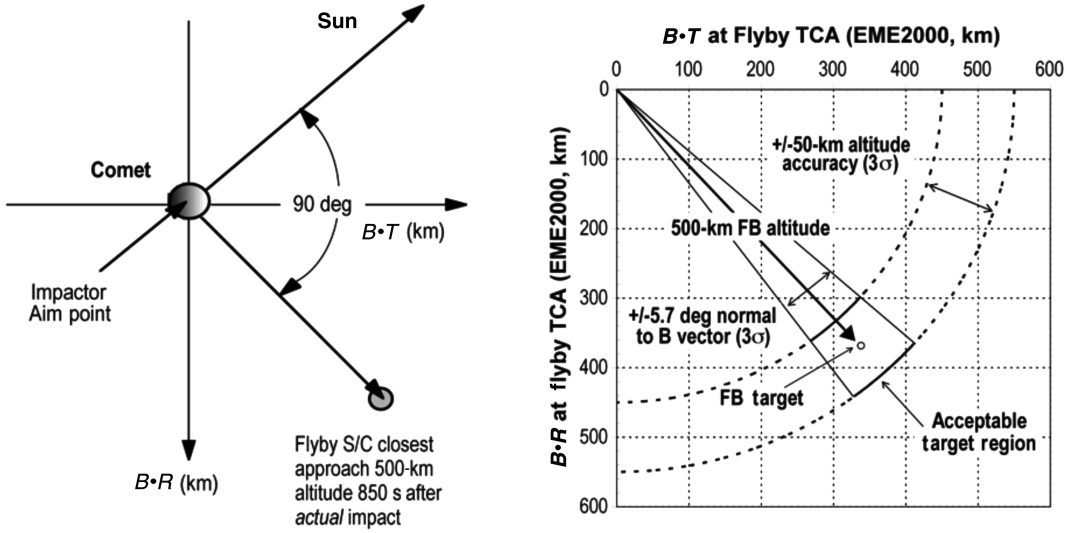

a) b)

Fig. 6 Flyby (FB) encounter target geometry: a) FB *B*-plane target geometry and b) FB delivery accuracy requirement (*B* plane is normal to the incoming inertial velocity direction).

TCM Schedule

The baseline mission design included six TCMs before impactor release, plus the large postrelease divert maneuver by the flyby spacecraft. Table 2 summarizes the placement and purpose for each maneuver. After launch, some TCMs were either deleted or moved to another time in response to new mission conditions. The reasons for these adaptive changes are summarized in Table 2 and discussed further throughout the paper.

Go/No-Go Criteria for Encounter TCMs

For the final two maneuvers near encounter, TCM-5 and the divert, we assigned two design cycles so that the first design could be uplinked and activated in case the later design could not be uplinked for some reason. We could set aside the second design if the first design met established criteria. It was very important for us to set clear and unambiguous go/no-go criteria for these maneuvers so that the right design could be confidently selected and promptly

Table 2 Planned and actual maneuver profile

Event	Planned or actual time	UTC epoch	Objectives
TCM-1	L + 20 days Actual delayed to L + 30 days	22 Jan. 2005, 19:00 11 Feb. 2005, 19:00	Removes statistical launch vehicle injection errors and targeting bias in declination of the outgoing asymptote (DLA error); adjusts TOI to the center of the 55-min observing window (4 July 2004, 06:00 UTC).
TCM-2	L + 57 days Deleted in flight; required trajectory corrections absorbed by TCM-3A	10 Mar. 2005, 19:00 ——	Statistical maneuver for timely removal of known trajectory errors resulting from orbit determination and/or TCM-1 execution error sources.
TCM-3A	E − 60 days	5 May 2005, 19:00	Changes Tempel 1 target impact time within the 55-min targeting window centered on 4 July 2005, 06:00 UTC, by up to ±27.5 min to enhance HST viewing; removes known trajectory errors. Uses in-flight update of Tempel 1 ephemeris based on latest ground-based astrometry, opnav images included, if comet detection has occurred.
TCM-3B	E − 20 days Delayed in flight to E − 11 days to use improved Tempel 1 ephemeris	14 June 2005, 19:00 23 June 2005, 19:00	Same objectives as TCM-3A. Makes final TOI adjustment for HST viewing of impact events; uses latest comet ephemeris based on combined ground-based and opnav astrometry.
TCM-4	E − 4 days Deleted in flight when TCM-3B moved to E − 11 days	30 June 2005, 06:00 ——	Provides required delivery accuracy for handover from ground navigation to impactor Autonav (assumes a healthy impactor). Corrects only *B*-plane delivery errors, not TOI (was not executed; objectives deferred to TCM-5).
TCM-5	E − 30 h (release − 6 h)	3 July 2005, 00:00	Provides final trajectory correction before impactor release; reduces size of impactor ITM-1. Corrects only *B*-plane delivery errors, not TOI.
TCM-6 (contingency)	E − 18 h	3 July 2005, 06:00	Contingency for TCM-5 (was not executed).
Impactor release	Impact − 24 h	3 July 2005, 06:00	Determines impactor release attitude; accounts for effect of spring release ΔV (34.8 cm/s) on impactor and FB spacecraft.
Divert maneuver	Release + 12 min	3 July 2005, 06:12	Slows FB spacecraft time of closest approach by 850 s and provides 500-km flyby distance to view impact events.
Divert trim (contingency)	Divert ΔV + 12 h	3 July 2005, 18:12	Contingency to remove unacceptable FB delivery errors following the divert maneuver (was not executed).

Table 3 Go/no-go criteria for maneuvers near encounter

Design DCO[a]	No-go criteria		Go criteria	
	Criteria with D.1 design and TCM-5	Action	Criteria with D.1 design and TCM-5	Action
Divert D.2 at E − 6 days	Flyby *B*-plane target error <20 km and flyby time delay[b] error < ± 10 s	D.2 design waived; use D.1 design	Flyby *B*-plane target error >20 km or flyby time delay [b] error > ± 10 s	Proceed with D.2 design
TCM-5.1 at E − 4 days	Flight system |B| < 5 km	5.1 design waived; proceed to 5.2 design	Flight system |B| > 5 km	Proceed with 5.1 design
TCM-5.2 at E − 42 h	Flight system |B| < 5 km	5.2 design waived	Flight system |B| > 5 km	Proceed with 5.2 design
Divert Trim at E − 20 h	Flyby *B*-plane target error <50 km and flyby time delay[b] error < ± 20 s	Divert trim is waived	Flyby *B*-plane target error >50 km or flyby time delay[b] error > ± 20 s	Proceed with divert trim design

[a]Tracking data cutoff (DCO) time for the maneuver design.
[b]The nominal time delay is equal to $[TCA_{flyby} - TOI_{impactor}] = 850$ s.

implemented during a busy encounter period filled with many critical events.

TCM-5 at E − 30 h was the final maneuver before impactor release at E − 24 h and was subject to the 30-km *B*-plane delivery accuracy required for handover to the impactor. Two design opportunities for TCM-5 to correct only lateral trajectory errors were designated TCM-5.1 and 5.2. Because these trajectory errors were statistical (unbiased), it was possible that TCM-5 would not be necessary. Similarly, there were two divert design opportunities: D.1 and D.2. Because the divert maneuver was an essential part of the baseline mission design, either D.1 or D.2 would be implemented. Plans were made for a single divert trim, designed for execution at E − 10 h, should the flyby divert maneuver fail to meet its 3σ *B*-plane and delay-time control requirements: 500 ± 50 km and $[TCA_{flyby} - TOI_{impactor}] = 850 \pm 20$ s, respectively.

Navigators have routinely used formal statistics to measure the orbit determination quality for comparison with specified delivery accuracy requirements. Usually, the *B*-plane 3σ delivery uncertainty ellipse centered on the current orbit estimate is compared with the chosen target. When the target is inside the delivery uncertainty ellipse, targeting accuracy requirements are satisfied. This strategy is most effective when the target body ephemeris is relatively well known (e.g., Mars). Formal delivery statistics relative to Tempel 1 were thought to be overly optimistic and additional conservatism was warranted given an unknown and ever-changing bias between the center of brightness observed in-flight and the center of mass [10,11]. "Scaling up" the solution uncertainties to account for this bias would have been somewhat arbitrary, subject to debate, and added unnecessary risk. We chose to remove formal statistics from the go/no-go decision-making process altogether and instead use straightforward best-estimate OD solutions for direct comparison with the target.

Table 3 summarizes the go/no-go criteria, including one major in-flight change in targeting philosophy: the minimum targeting error that would require the execution of TCM-5 was reduced from 30 to 5 km. This change offered two important advantages:

1) It improved the delivery accuracy for the divert maneuver to reduce the probability that a divert trim would be required (described later).

2) It reduced the targeting responsibility of the impactor Autonav system by making ITM-1 smaller.

The go/no-go criterion for executing TCM-5 became more conservative, but also very clear and simple: TCM-5 would be needed only if the required *B*-plane target correction was greater than 5 km.

The encounter TCM timeline updated in flight proved to be a significant improvement over earlier designs [12], because our schedule was more tractable and we had well-defined success criteria and decision-making processes. The new strategy also allowed TCM-4, planned at E − 4 days, to be eliminated. As noted in Table 2, TCM-4 was originally subject to the 30-km prerelease delivery accuracy requirement for handoff to the impactor Autonav. The earlier plan would have allowed us to cancel TCM-5 if TCM-4 satisfied the 30-km delivery accuracy. But now, we were not assured of achieving the 5-km delivery accuracy with TCM-4 without also including TCM-5 because of expected Tempel 1 ephemeris uncertainties at E − 4 days (the MRI resolution at E − 4 days was 36 km/pixel, compared with an estimated nucleus diameter of 5–10 km).

The in-flight change in TCM-5 targeting philosophy also had important implications for the flyby divert maneuver because its delivery accuracy was tied directly to the delivery accuracy of TCM-5. There was not enough time for us to update the divert design to reflect achieved TCM-5 performance, and so any TCM-5 targeting error would introduce the same error as a bias in divert maneuver targeting. With TCM-5 targeted within 5 km of an intercept trajectory instead of 30 km, we expected the divert execution errors to be the dominant source of flyby delivery errors.

Because the divert maneuver was deterministic, we could complete designs for both D.1 and D.2 *before* the final TCM-5 design and implementation. This convenient circumstance allowed our operations workload during encounter to be more evenly distributed, while also allowing time for valuable backup designs. However, these divert designs depended on the successful execution of TCM-5. To insure that the flyby would meet its targeting objectives, we added a contingency TCM-6 at E − 18 h as a replacement for a failed TCM-5.[§§]

We designed, uplinked, and activated the divert D.1 using a 48-h design schedule beginning at E − 28 days, as shown in Fig. 7. Also, we fully tested and validated the D.1 design as part of the final operational-readiness test (ORT-11). We used the D.2 update to check the validity of the D.1 design based on more recent comet-relative orbit determination estimates available at E − 6 days.

The decision-making processes we adopted worked very effectively and should be given serious consideration by future navigators faced with similar circumstances. However, the specific strategies should be defined and tested much earlier than they were for Deep Impact. Every mission includes in-flight ORTs that must compete for human resources and time with ongoing mission operations, and the added risks of significant in-flight changes to the baseline plan should be avoided.

TCM ΔV Budget

All TCMs scheduled before impactor release were to be achieved within a ΔV_{99}[¶] allocation of 65 m/s, requiring 27 kg of fuel. Preflight maneuver analyses that reflected predicted launch vehicle injection accuracy, plus errors due to orbit determination and maneuver execution, showed design margin, requiring a mission ΔV_{99} of 60 m/s and 25 kg of fuel, with TCM-1 at L + 20 days. The deterministic flyby divert maneuver following impactor release at E − 24 h required 102.5 m/s, mostly to provide the 850-s time

[§§]This contingency would result in a late impactor release at E − 10 h, followed by a divert maneuver of 246 m/s.

[¶]ΔV_{99} equals the 99% value from the distribution of total maneuver ΔV estimated by simulating 5000 sample missions.

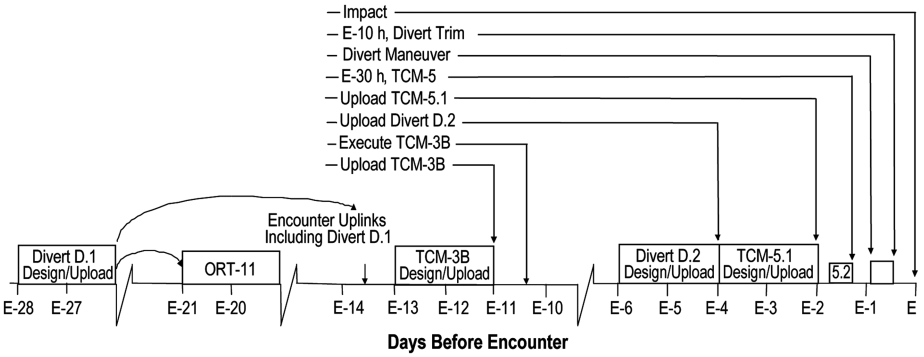

Fig. 7 Encounter-phase maneuver timeline.

delay; the ΔV_{99} allocation was 105 m/s including expected divert execution errors. A total of 51 kg of propellant was required for the baseline mission. The resulting fuel margin of 34 kg could support a contingency impactor release as late as E − 9 h, while retaining the capability to provide the flyby divert ΔV required for an 850-s TCA delay.

Shortly before launch, TCM-1 was delayed until L + 30 days to allocate more time for planned early flight system calibration activities. This delay increased the prerelease ΔV_{99} estimate from 60 to 72 m/s (Table 4), including a 6.3-m/s deterministic component at TCM-1 to remove a known launch vehicle targeting error (discussed later). Our mission fuel margin dropped from 34 to 29 kg, requiring a contingency divert maneuver no later than E − 10 h.

TCM Pointing Constraints

Each TCM was subject to geometric pointing constraints imposed by performance limitations of the power, thermal, and telecom subsystems and the flight system instruments (Fig. 3). The power constraint limited the angular offset of the solar array normal ($+Y$ axis) from the sun direction, whereas the thermal constraint prevented excessive solar illumination on critical flight system surfaces. The power constraint became more restrictive with solar distance, which steadily increased after launch (Fig. 2). The power management objective was to limit battery depth of discharge to an acceptable level during a TCM turn–burn–turn sequence. Thermal constraint violations triggered the use of radiators that in turn increased power consumption. In general, thermal concerns were mitigated when battery performance levels (i.e., power requirements) were judged acceptable. The telecom constraints during TCMs limited the orientations of both the HGA and LGA signal beam widths with respect to the direction to Earth-based antennas. Our goal was to take advantage of the higher signal strength and data rates available with the HGA whenever possible; if not, use one of the two LGAs. The HGA was available when Earth-pointing could be maintained within the physical Y- and Z-gimbal limits.*** Either LGA-1 (along $+Y$) or LGA-2 (along $-Y$) could be used when the Earth direction was within an acceptable angular offset from these axes. The LGA constraint limits varied with trajectory position, Earth distance, ground-based antenna used (34 or 70 m), and the required data rate. The flight system instruments included three star-trackers plus the HRI, MRI, and ITS cameras. Each of these instruments required protection from sunlight within a specified keep-out cone centered on its bore sight [12].

Our need for TCM constraint assessment and mitigation procedures had been completely overlooked by the flight team until it became evident during an ORT for TCM-1 in August 2004. Subsequent maneuver analyses [12] indicated a high probability that at least one pointing constraint would be violated for every TCM. To address this concern, navigators and spacecraft team personnel collaborated to define the appropriate constraint limits, to develop methods of quickly detecting violations, and then to determine the proper response to any violation. When a TCM constraint was violated, we planned to split the required maneuver into two constraint-free components executed a day apart to achieve the same target correction as the original maneuver. We developed new software and modified maneuver design procedures to detect constraint violations and to define acceptable solutions. These implementation tasks became an unexpected and time-consuming addition to an already busy flight team workload.

The mission ΔV_{99} required to satisfy the TCM pointing constraints is summarized in Table 5. Whenever a Monte Carlo sample TCM ΔV violated a pointing constraint, a pair of constraint-free maneuvers (parts A and B) was executed. When no constraint was violated, the single maneuver was executed. The cost of satisfying TCM pointing constraints increased the prerelease ΔV_{99} estimate from 72 to 79 m/s and lowered the fuel margin from 29 to 27 kg. This fuel margin allowed impactor release no later than

Table 4 ΔV statistics for baseline maneuver design without maneuver constraints [12]

TCM	Epoch	Deterministic ΔV, m/s	Statistical ΔV, m/s			
			Mean	1σ	99%	Cumulative mission ΔV_{99}
TCM-1	L + 30 days	6.3	22.4	13.5	63.0	63.0
TCM-2	Mar 10, 2005	——	0.3	0.2	0.9	63.9
TCM-3A	E − 60 days	3.2	3.2	0.07	3.4	67.1
TCM-3B	E − 20 days	4.4	4.4	0.1	4.7	71.6
TCM-4	E − 4 days	——	0.3	0.2	0.8	71.9
TCM-5	E − 30 h	——	0.1	0.06	0.3	72.0
Divert	Release + 12 min	100.4	100.9	0.5	101.6	72.2
Divert trim	E − 12 h	——	0.3	0.2	0.7	172.5
Total ΔV		114.3	131.6	13.7	172.5	172.5

***Hardware limits for the HGA gimbals were $-68\,\text{deg} \le \text{HGA-}y \le +68\,\text{deg}$ and $-80\,\text{deg} \le \text{HGA-}z \le +64\,\text{deg}$; during operations tighter software limits were used to provide a performance margin against these hardware limits.

Table 5 ΔV statistics including maneuver constraints [12]

TCM	Epoch (L+ or E− days)	Deterministic ΔV, m/s	Statistical ΔV, m/s			
			Mean	1σ	99%	Cumulative mission ΔV_{99}
TCM-1A	L + 30	6.3	19.9	11.5	55.2	55.2
TCM-1B	L + 31	——	3.9	5.6	50.3	68.7
TCM-2A	10 Mar. 2005	——	0.3	0.2	0.9	69.4
TCM-2B	11 Mar. 2005	——	0.04	0.08	0.8	69.5
TCM-3A-1	E − 60	3.2	3.2	0.07	3.4	72.7
TCM-3A-2	E − 59	——	0.03	0.04	3.4	72.8
TCM-3B-1	E − 20	4.4	4.4	0.1	4.7	77.4
TCM-3B-2	E − 19	——	0.01	0.01	4.7	77.4
TCM-4A	E − 4	——	0.5	0.2	1.0	78.0
TCM-4B	E − 3	——	0.05	0.1	1.0	78.0
TCM-5A	E − 30 h	——	0.9	0.6	2.8	79.0
TCM-5B	E − 30 h	——	0.06	0.05	0.2	79.0
Divert	Release + 12 min	100.4	100.4	0.5	101.6	170.0
Divert Trim	E − 12 h	——	0.3	0.2	0.8	179.4
Total ΔV		114.4	134.0	15.3	179.4	179.4

E − 12 h while providing the required 850 s delay in the time of flyby closest approach. This evaluation process was needed and successfully used for TCM-1 design [12] (discussed later), but the experience taught some very important lessons.

Early flight system design, including placement of instruments and antennas, effectively addressed and satisfied pointing constraints for the planned cruise attitudes (Fig. 3b), especially for the critical encounter phase. However, expected deviations from these very restricted flight attitudes for TCM execution had not been carefully examined. A formal requirement placed on the flight system and the flyby stated they "...shall be capable of applying a velocity increment...in any inertial direction." This requirement could not be met. A timely prelaunch audit to validate and verify this requirement was needed, but one did not occur. Future missions can avoid similar awkward surprises and be much better prepared for testing and flight operations by determining applicable TCM pointing constraints early in the mission and spacecraft design processes, certainly no later than the flight system preliminary design review. This process is particularly important to assure adequate TCM fuel margins and to develop appropriate mission operations tools and procedures.

Orbit Determination Design

Ground-based orbit determination for all mission phases used coherent radiometric Doppler and range data acquired by the NASA Deep Space Network (DSN). These traditional radiometric data types were augmented by delta-differential one-way range (ΔDOR). When combined with Doppler and range, ΔDOR provides a measurement orthogonal to the line of sight to minimize the effects of nongravitational modeling errors, thereby greatly increasing our confidence in the overall OD accuracy. Most important, we were assured of a very stable radio-only heliocentric reference trajectory needed when opnav images were combined with ground-based astrometry measurements during the comet ephemeris improvement process. Figure 8 shows that our actual tracking hours were greater than originally planned due to a compressed mission timeline imposed by a delayed launch and busier-than-planned calibration activities. This unplanned increase in tracking directly reflects an overall increased workload on the flight team, but the additional tracking data were beneficial to navigation.

Our primary OD objectives were to support the impactor and flyby target delivery accuracy requirements specified earlier and the design and reconstruction of each TCM and to provide a spacecraft ephemeris to seed the encounter sequences for Autonav onboard both the impactor and flyby. Major OD tasks included modeling solar radiation pressure, accounting for as-flown and predicted spacecraft attitude, and estimating and predicting the effects of propulsive momentum desaturation maneuvers.

Early orbit determination depended solely on radiometric and ΔDOR observations to define the heliocentric trajectory. The first

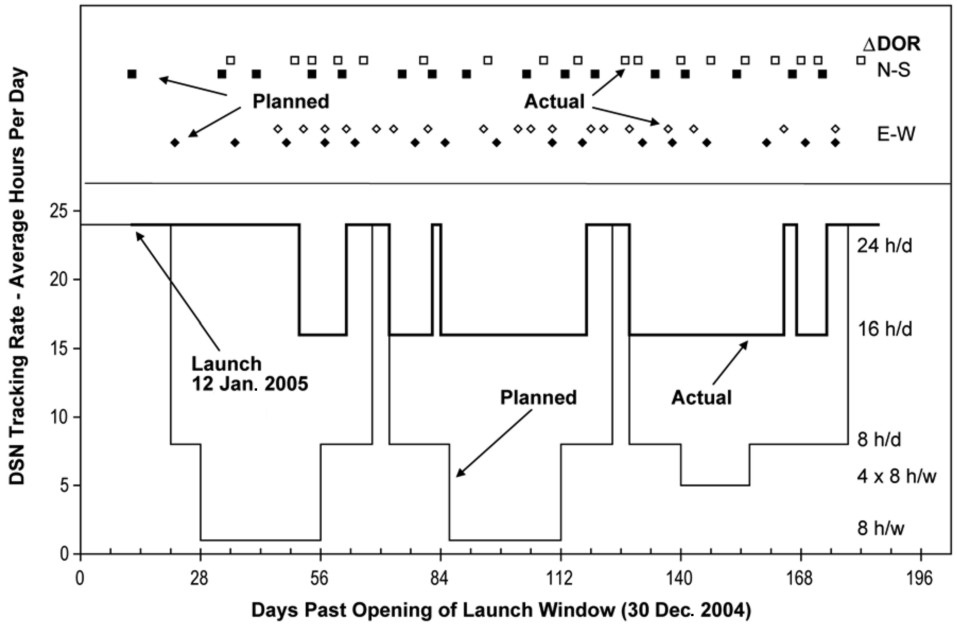

Fig. 8 Planned and actual DSN tracking schedule.

opnav images with the HRI were expected near E − 120 days (6 March 2005), but delays in calibration activities postponed the first MRI image until 25 April 2005 (described in the next section). The opnav data allowed estimates of the comet-relative spacecraft trajectory and the Tempel 1 ephemeris. These measurements were also used in the ground-based Tempel 1 ephemeris development process, described later.

Solar radiation pressure was expected to be the primary error source for both orbit determination and prediction. A new solar pressure model, developed for Deep Impact by BATC using finite element modeling, defined tabular values of body-fixed Cartesian vectors of (area times reflectivity) as functions of solar azimuth in the body frame and the HGA Z-gimbal position for Earth-pointing (Fig. 3b). This model defined the spacecraft projected area very accurately at each discrete attitude, whereas alternative component models can be less precise when not accounting for shadowing. However, the finite element model was valid only for the range of flight attitudes planned for interplanetary cruise. For other attitudes, such as periodic opnav imaging sequences beginning 25 April 2005, and the near-continuous comet-pointing attitudes during the final seven days, we used component models based on preflight estimates of the flight system surface areas and the specular and diffuse coefficients of various body components [10]. Frequent performance comparisons between the two models helped validate solar pressure modeling and maintain OD solution consistency.

A second OD and trajectory prediction error source concerned propulsive desats needed to negate angular momentum buildup. As described earlier, the flight system uses reaction wheels and RCS thrusters for attitude control. Momentum management is accomplished by maintaining the CP in near-alignment with the CM. In actual flight, the momentum buildup was much faster than prelaunch predictions, and the workload associated with executing coupled desats was not supportable. As a result, about two desats per week were needed compared with the predicted once per month, and only uncoupled desats with an attendant ΔV were performed. Consequently, desats were a larger-than-anticipated source of trajectory perturbation. We required additional flight team effort [10] to model and predict the effects of future desats on trajectory prediction accuracy. However, the availability and use of frequent ΔDOR observations helped keep our radio-only trajectory very well-determined so that there was little consequence to the increased desat frequency and to errors in predicting their effects on the flight system trajectory.

Optical Navigation Design

The baseline mission design planned to use the HRI to acquire opnav images of Tempel 1, with the MRI serving as a backup. Initial data acquisition for navigation was planned near E − 60 days when the flight system was 50 million km from the comet. At this distance, one HRI pixel subtended 100 km, much larger than the estimated nucleus diameter (less than 10 km). However, this resolution was still adequate to support orbit determination and to provide onboard data for the comet ephemeris improvement campaign, because center-finding on point sources can be accurate to 0.1 pixel. However, the first HRI pictures, taken for alignment purposes just two days after launch, revealed an uncorrectable focus problem arising from a faulty prelaunch alignment procedure. Our Opnav imaging sequences were then completely replanned to use the MRI, with its fivefold-lower resolution of 10 μrad/pixel. It would not be until E − 12 days that the MRI could provide the same 100 km/pixel resolution that the HRI was expected to provide at E − 60 days. As a result, comet-relative orbit determination and comet ephemeris accuracy improvements based on combined ground-based and opnav astrometry were forced to operate on a compressed and sometimes very hectic timeline.

The nominal opnav imaging profile that began with key calibration activities is summarized in Table 6. More information about individual calibrations is available from Owen et al. [11].

Flight system temperature constraints limited comet imaging between E − 60 and E − 7 days to 15-min opportunities (four pictures) every 4 h. Beginning at E − 7 days, opnav imaging was continuous except near key events such as TCMs, impactor release, and the flyby divert maneuver.

The Opnav analysts used a suite of six data reduction techniques, which we called "the gang of six," to attempt to locate the nucleus in each image [11]. Some of these data reduction methods were first introduced and successfully used in 2004 during the Stardust flyby of comet 81P/Wild 2 [5]. Each technique used a different method to minimize the contribution of the coma from that of the nucleus. The Opnav analysts recommended the best technique for using opnav data in the orbit determination process. However, orbit determination was always performed using opnav data from all six data reduction techniques to allow routine comparisons.

Tempel 1 Ephemeris Development

When the Deep Impact project began in 2000, ESA's 1986 Giotto mission to comet 1P/Halley was the only spacecraft to have

Table 6 Baseline optical navigation imaging profile [11,13]

Time from encounter	Picture rate	Purpose
120 to 60 days (first comet detection)	48 images per week	Ephemeris verification Camera calibrations Ground software testing
60 days	24 images per day	Ephemeris verification Camera calibrations Ground software testing
50 days	24 images per day	Ephemeris improvement Coma and nucleus brightness estimation Ground image processing test Centroiding accuracy assessment
20 days	24 images per day	COB/COM[a] resolution Rotational period estimate Coma and nucleus brightness estimation Jet periodicity established Possible nucleus detection
10 days	3 HRI image/3 min	Support of TCM-4 at E − 4 days COB/COM resolution
4.25 days	3 HRI image/9 min	Support of baseline TCM-5 at E − 30 h
E − 30 h	3 HRI image/9 min	Support contingent delay of TCM-5 for potential impactor anomaly
E − 25 h	Last high-rate opnav image	——
E − 22:48 to E − 18 h	1 every 20 min	Support trim deflection maneuver
E − 17 to E − 3 h	2 per hour	Star-trackers attitude-bias estimate
E − 18 to E − 2 h	1 per 2 h with HRI, ITS	Trajectory reconstruction for science

[a]COB is the center of brightness and COM is the center of mass.

navigated a close-up flyby of a comet. Muench et al. [14] reported the Halley ephemeris accuracy improvements needed to achieve the 600-km flyby within a 1σ uncertainty of ± 40 km. The ambitious Deep Impact targeting objectives required an even greater improvement in Tempel 1's ephemeris.

Comet Tempel 1 was first discovered by Ernst Wilhelm Liebrecht Tempel in 1867 when it passed within 0.6 AU of Earth and 1.6 AU of the sun [15]. Close flybys of Jupiter in 1881 caused this Jupiter family comet to be lost until Brian Marsden in 1963 predicted its return in 1967 and 1972 [16]. Observations in 1972 confirmed that a single image taken by Elizabeth Roemer on 8 June 1967 was of comet 9P/Tempel 1, so named as the ninth periodic comet discovered.

The astrometric database used in the Tempel 1 ephemeris development process for Deep Impact begins with the Roemer observation taken on 8 June 1967. Table 7 summarizes the key characteristics of nine ephemeris deliveries provided by Chesley and Yeomans [17] between June 2000 and September 2005 that were used to support Deep Impact navigation design and flight operations activities. This list identifies the number of observations, the data arc length, and the primary use for Deep Impact navigation. The solution naming convention is as follows: K means century 2000, the first two digits after K define the year of the delivery, the third digit defines the number of apparitions included in the solution data arc, and the number after the slash defines the solution sequence number. For example, K007/24 was the 24th solution delivered in the year 2000 using data from seven apparitions.

A diverse community of professional and amateur astronomers acquired images of Tempel 1 using a wide range of imaging capabilities and data reduction techniques [18,19]. The data consisted entirely of angular observations of right ascension (RA) and declination (DEC). Chesley and Yeomans [17] reported that ephemeris development using these data was very challenging for several reasons. First, nongravitational accelerations resulting from random rocketlike outgassing of materials from the surface were difficult to model and even more difficult to predict. Also, astrometric measurement errors were difficult to model, particularly the systematic errors.

Modeling of nongravitational accelerations has improved in recent years, but the model is still based primarily on the assumption in 1973 by Marsden et al. [20] that the related forces varied with heliocentric distance. More recent attempts to model discrete body-fixed jets have met with some success, but they often have some difficult-to-model stochastic component. These problems lead to difficulties in deriving credible ephemeris statistics. Astrometric measurement errors make things even worse. These errors occur because the comet nucleus is hidden within the coma, making it difficult to obtain a direct measure of the nucleus position. This problem leads to observational biases either because the center of brightness is offset from the center of mass or because data reduction techniques cannot adequately locate the center of brightness.

The estimation uncertainties mapped to the Tempel 1 B plane are listed in Table 8 for each of the nine ephemeris deliveries. The B-plane intercept and the uncertainties for these deliveries are compared in Fig. 9 with respect to the final ephemeris delivery on 28 September 2005 (K051/17). Deliveries before 2 May 2005 (K052/7), shown on the right side of Fig. 9a, exhibit some inconsistencies due to measurements biases. The K052/7 delivery was the first to include opnav measurements, and these important additions contributed to a B-plane shift of more than 900 km (Fig. 9b). These astrometric measurements provided good information normal to the observer's line of sight, but they were less sensitive along the line of sight (S direction). With a comet-relative spacecraft velocity of 10.2 km/s, the comet ephemeris uncertainties in the S direction resulted in 1σ TOI uncertainties that varied between 17 and 41 s, as shown in Fig. 10. The largest uncertainties were reported for solution K052/7, for which measurement biases were evident for nearly half of the ground-based astrometric data [17].

The procedures we used to combine ground-based and opnav data are described in Fig. 11. The opnav data are accompanied by a heliocentric spacecraft ephemeris based on only radiometric tracking data: Doppler, range, and ΔDOR. Spacecraft position vectors at each opnav observation epoch served as geocentric station locations in the overall astrometric data fitting process. This procedure relies on the

Table 7 Schedule of Tempel 1 ephemeris deliveries [17]

		Observations					
Solution ID	Delivery date	Ground	Opnav	Simulated	Date arc (opnav arc)	Use by Deep Impact	Opnav included?
K007/30	6/5/00	528	——	——	6/8/67 to 5/11/00	——	——
K007/39	8/24/01	686	——	21	6/8/67 to 12/27/00	——	——
K058/3	6/29/04	706	——	61	6/8/67 to 12/26/03	Prelaunch design and analysis	No
K054/6	1/10/05	573	——	62	10/87 to 12/04	TCM-1 on 2/11/05	No
K053/11	2/16/05	695	——	47	1/21/93 to 2/7/05	TCM-2 on 3/10/05	No
K052/7	5/2/05	788	30	32	8/3/94 to 4/27/05 (4/25.89/05, over 8 min)	TCM-3A on 5/5/05	Yes
K052/32	6/21/05	1022	201	——	8/3.5/94 to 6/20.5/05 6/3.05/05 to 6/19.89/05)	TCM-3B on 6/23/05	Yes
K051/9	7/1/05	671	909	——	10/1.5/03 to 6/29.5/05 (5/7.7/05 to 6/29.5/05)	TCM-5 on 7/3/05	Yes
K051/17	9/28/05	922	3956	——	10/1.5/03 to 7/4.9/05 6/29.489/05 to 7/4.247/05)	Final ephemeris delivery	Yes

Table 8 Tempel 1 ephemeris estimation accuracies [17] (solution 1σ uncertainties mapped to 4 July 2005, 05:45 ET)

		B-plane coordinate system (EME2000)				B-plane ellipsoid semi-axes		
Solution ID	Delivery date	R, km	T, km	S, km	Time of flight, s	Major, km	Minor, km	Θ[a], deg
K007/30	6/5/00	91	79	186	18	111	46	39
K007/39	8/24/01	90	73	171	17	108	43	37
K058/3	6/29/04	101	79	205	20	113	60	58
K054/6	1/10/05	102	140	278	27	154	79	151
K053/11	2/16/05	104	112	281	27	138	65	138
K052/7	5/2/05	205	122	419	41	228	72	117
K052/32	6/21/05	52	87	180	17	98	26	118
K051/9	7/1/05	43	71	178	17	69	40	86
K051/17	9/28/05	0.54	0.55	6.5	0.6	0.59	0.5	47

[a]Orientation angle of the B-plane ellipse major axis measured positive clockwise from the $+T$ axis.

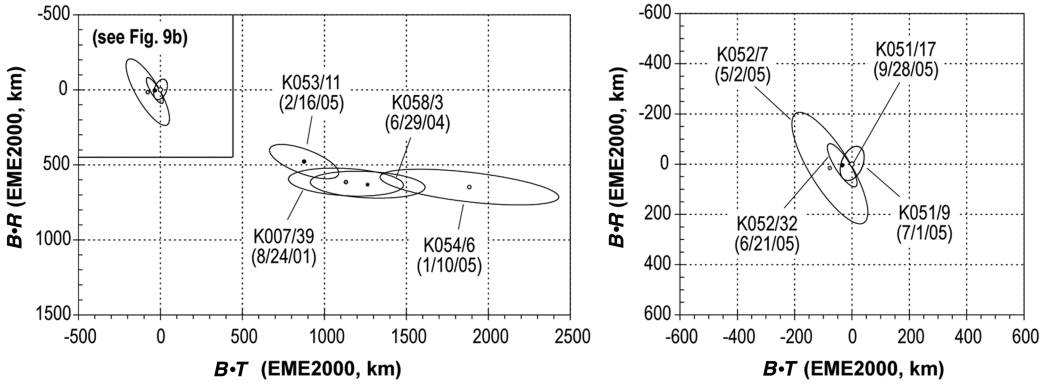

a) b)

Fig. 9 Evolution of Tempel 1 ephemeris *B*-plane solutions and delivery dates, plus 1σ uncertainties referenced to final delivery K051/17: a) 24 August 2001 to 16 February 2005 and b) 2 May 2005 to 28 September 2005.

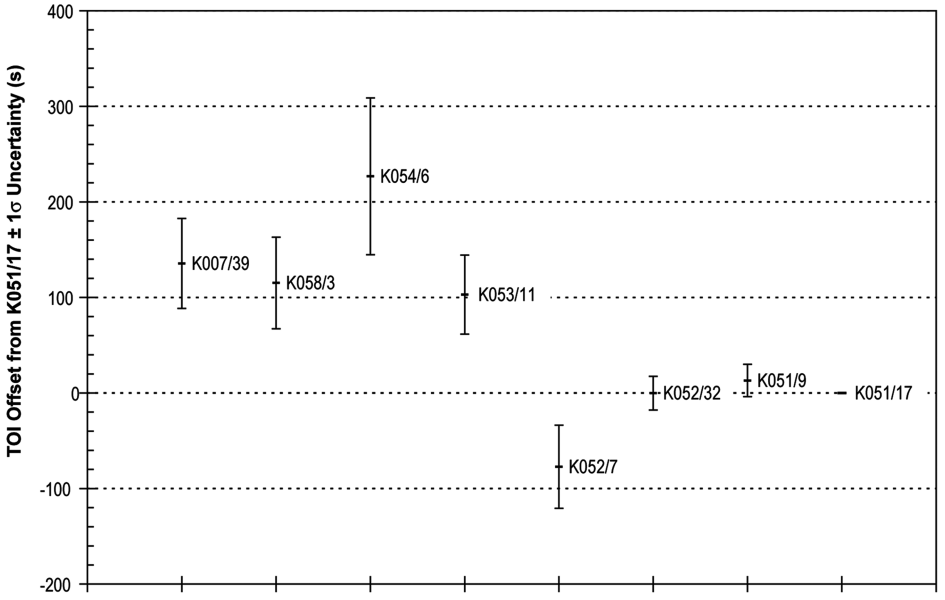

Fig. 10 Tempel 1 ephemeris uncertainty in the *S* direction.

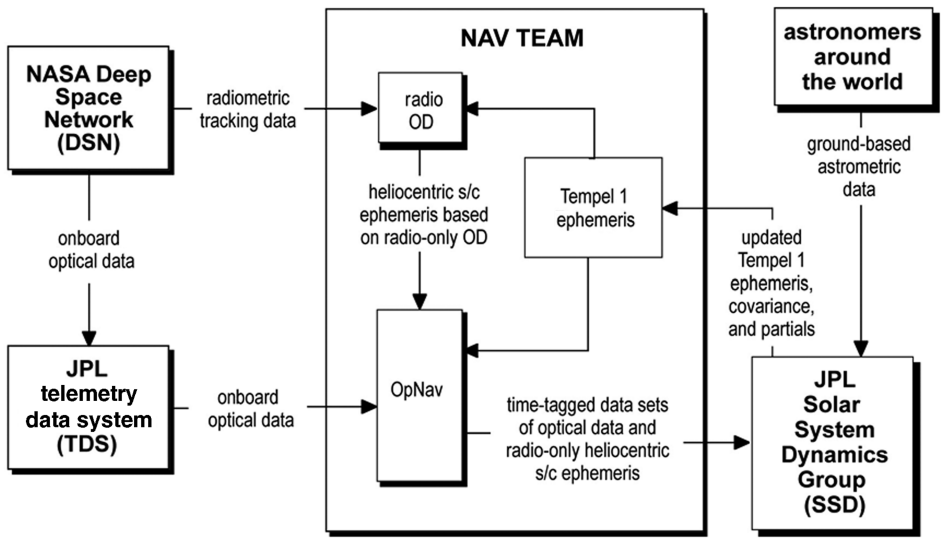

Fig. 11 Interfaces and procedures for using opnav data in comet ephemeris update process.

Table 9 Comparison of specified (DTO[a]) and adjusted (BET) launch vehicle target parameters at the TIP.

Launch date and time: 12 January 2005, 18:47:08.571 UTC Launch azimuth: 101 deg TIP time: 12 January 2005, 19:25:00.100 UTC			
Launch vehicle target parameters	Specified target parameters at the TIP (DTO)	Boeing adjusted target parameters (BET)	TCM-1 correction at L + 30 days
C_3, km^2/s^2	10.8720	10.8577	$\Delta V = 6.3$ m/s to correct the launch vehicle's DLA targeting error
RLA, deg	199.3073	199.3089	
DLA, deg	−2.9596	−2.8248	
$B \cdot R$ at Tempel 1 TCA, km	0	−60, 211	
$B \cdot T$ at Tempel 1 TCA, km	0	10,083	
TCA at Tempel 1 (UTC)	7/4/05, 05:52:34	7/4/05, 06:22:43	

[a]Detailed test objectives.

Table 10 Comparison of specified, targeted, and achieved launch vehicle parameters at the TIP

Parameter	Specified target (DTO[a])	Boeing target (adjusted BET)	Expected dispersions, 1σ	Achieved target	Achieved minus DTO
C_3, km^2/s^2	10.8720	10.8577	0.0722	10.7554	−0.1166 (1.6σ low)
DLA, deg	−2.9596	−2.8248	0.1236	−2.8416	−0.1180 (0.95σ low)
RLA, deg	199.3073	199.3089	0.1956	199.3849	0.0776 (0.4σ high)

[a]Detailed test objectives.

comet ephemeris development process to detect and resolve inconsistencies between ground-based and opnav astrometric measurements.

Navigation Performance

Launch Phase

Deep Impact was successfully launched on 12 January 2005, on the 14th day of the launch period. An initial delay of nine days provided additional time to more thoroughly test spacecraft flight software. A second delay resulted when Boeing replaced the Delta II 7925 interstage ring. Also, shortly before launch, Boeing discovered an inconsistency in the launch vehicle second-stage modeling that meant the required targeting parameters could not be achieved with their design trajectories.

Table 9 compares the specified target values defined at the target interface point (TIP) with the Boeing best-estimate trajectory (BET). The TIP epoch is defined as 10 min after nominal Stage-III ignition. There was not enough time to fully correct these targeting errors; instead, Boeing adjusted liftoff time to compensate for the targeting discrepancy in the right ascension of the outgoing asymptote (RLA). The spacecraft would then correct the error in the declination of the outgoing asymptote (DLA) as part of TCM-1 at L + 30 days. This was a feasible targeting solution, because the available flight system propellant margin could accommodate the additional 6.3 m/s needed at TCM-1 to correct the DLA targeting error of 0.13 deg.

Table 10 shows that the achieved target parameters at the nominal TIP time matched the Boeing-adjusted BET very well in RLA and DLA, but the C_3[†††] was 1.6σ low. Correction to the Tempel 1 impact aim point and TOI required a TCM-1 of 27.7 m/s, including the cost to correct the launch vehicle's DLA targeting error.

Two competing contingency situations that affected navigation were encountered soon after launch. The first required timely determination of the achieved injection trajectory in the presence of the 1.6σ C_3 injection error to update pointing predictions for the second scheduled DSN tracking pass, over Madrid. The second contingency concerned the flight team's response to an unexpected safing event and its effect on the early injection orbit determination process.

The flight system unexpectedly entered sun-safe mode shortly after separation from the launch vehicle. The sun-safe mode points the $+Y$ axis at the sun while rotating about $+Y$ once every 4 h to minimize thermal concerns while also reducing momentum buildup. The default telecom configuration had coherency disabled, and so only angles and one-way Doppler data acquired by the initial 4-h Canberra pass were available for early orbit determination. A timely update of the station-pointing predictions was needed for the upcoming Madrid pass, but we could not confidently determine the achieved trajectory in the presence of the observed injection errors without the benefit of coherent two-way tracking. This situation put at risk a successful acquisition by Madrid at a time when the flight system remained in safe mode without a clear timeline for recovery. In parallel, the flight team was actively determining the cause of the safing event. A careful review process concluded that fault-protection software had detected propulsion system temperatures higher than expected; resetting the fault limits to the intended values would correct the problem. To initiate safe-mode recovery, the flight system was commanded to coherent two-way tracking just 20 min before the end of the Canberra pass. Orbit determination using these data was promptly followed by an update of the antenna-pointing predictions, just in time for a successful acquisition by Madrid.

Safe-mode configurations typically power off all but the essential spacecraft systems; the Deep Impact launch sequence design reflected that procedure. However, use of this strategy also meant that the orbit determination accuracy needed to confidently update antenna-pointing predictions at Madrid was at risk while the flight team determined why safe mode had occurred. In hindsight, the project would have done well to balance these risks by more thorough planning before launch. Future consideration should be given to configuring safe mode at launch with coherency enabled so that two-way tracking data would remain available for early injection orbit determination. Once the injection orbit has been confidently established, the safe-mode telecom configuration can be restored to the preferred coherency disabled. For purposes of tracking station acquisition in the presence of large injection errors, the orbit becomes adequately determined when a small amount of coherent tracking data from the second scheduled tracking pass is included in orbit determination.

Cruise Phase

Soon after launch, a series of planned activities began to check out the flight system and to calibrate key subsystems and instruments. Just two days after launch, the first HRI images revealed a focus problem that was later determined uncorrectable following several unsuccessful bake-out sessions. This meant the opnav imaging campaign had to be completely replanned to use the backup MRI. Orbit determination continued in preparation for TCM-1 at L + 30 days on 11 February 2005.

[†††]The parameter C_3 is used to measure launch vehicle performance, equal to twice the energy per unit mass; $C_3 = v^2 - 2\mu/r$, where v is the velocity in km/s, μ is the gravitational potential in km^3/s^2, and r is the magnitude of the geocentric radius vector in kilometers.

The project preferred that TCM-1 be executed using the HGA to gain valuable telecom experience before the critical flyby divert maneuver scheduled soon after impactor release. Unfortunately, the required ΔV pointing direction was opposite from the Earth direction, and so the HGA was not available. The only alternative was LGA-2, but its Earth-relative geometry offered only marginal signal strength. The $-Y$ axis offset from the Earth direction was 76.8 deg, exceeding the 73.5-deg value needed at TCM-1 for a telemetry data rate of 2 kbps. Rolling the spacecraft $+X$ axis about the required ΔV direction could not improve the LGA-2 geometry without also violating the 55-deg power constraint ($+Y$ offset from sun direction). Even so, this marginal case could have been selected for implementation, but all remaining TCMs before the flyby divert were statistical, with low probabilities of providing the Earth-viewing geometry needed to assure availability of the HGA.

We chose an alternate design strategy to improve the TCM-1 telecom geometry by biasing TCM-2 (10 March 2005). Our selection of RA = 23.9 deg and DEC = 54.4 deg for the biased TCM-2 pointing direction provided constraint-free geometry for TCM-2, including use of the HGA. The trade space summarized in Table 11 shows the effect of TCM-2 magnitude on TCM-1 maneuver ΔV and constraint parameters. A TCM-2 magnitude of 4 m/s assured constraint-free geometry in the presence of 3σ trajectory prediction errors. This design resulted in a TCM-1 magnitude of 28.6 m/s with a pointing direction that improved the telemetry signal via LGA-2. The additional ΔV cost for this strategy was 4.9 m/s. The resulting power-constraint violation for TCM-1, requiring brief use of batteries, was judged acceptable.

The TCM-1 execution errors were expected to be the dominant source of postmaneuver trajectory errors. However, orbit determination indicated that the achieved maneuver parameters closely matched the design values (Table 12). This maneuver performance was achieved as ADCS software and three-axis accelerometers teamed with an innovative taper strategy to reduce the firing duty cycle during final thrusting, thereby allowing the achieved ΔV vector to precisely "sneak up on" the design vector. The primary motivation for this software capability was to limit execution errors for the large flyby divert maneuver after impactor release, but this control technique proved very effective for all TCMs.

Approach Phase

The approach phase between E − 60 and E − 10 days marked the scheduled start of opnav imaging and also included TCMs 3A and 3B. The excellent TCM-1 performance, plus an acceptably small cost to delay TCM-2, allowed us to cancel TCM-2 and absorb the modest trajectory corrections with TCM-3A. We found these favorable trajectory conditions very helpful, because ongoing instrument calibrations needed the full attention of the flight team.

The primary objectives of TCM-3A were to take advantage of the first Tempel 1 ephemeris update based on both ground-based and opnav images and to adjust the target time of impact (TOI) on 4 July 2005 to a value selected by the Deep Impact science team. The science team had defined a 55-min observing window starting at nautical twilight +10 min at Mauna Kea, Hawaii, for viewing from the Keck Observatory. The window exit time matched the Goldstone view period set at a 15-deg elevation. One role of TCM-1 had been to target near the center of this observing window so that TCM-3A could later refine the target TOI to enhance impact viewing by the Hubble Space Telescope (HST). Following recommendations from HST based on predicted atmospheric drag estimates, the science team selected a TOI target of 05:52 Earth receive time (ERT), while retaining the option to make a final adjustment at TCM-3B on 23 June 2005. Using Tempel 1 ephemeris update K052/7, the flight team elected to target TCM-3A 10 min earlier to assure a constraint-free TCM-3B using the HGA [12]. As was observed for TCM-1, the achieved TCM-3A maneuver parameters were not measurably different from their design values (Table 12), further increasing our confidence that continued good performance remained a reasonable expectation for the remaining TCMs.

TCM-3B at E − 11 days was the final prerelease maneuver designed to correct both TOI and B-plane targeting errors. The science team chose to retain the original target TOI of 05:52 ERT. The required B-plane corrections depended on estimates of the Tempel 1 ephemeris expected to include opnav images acquired by the MRI. However, orbit determination solutions using these opnav were inconsistent, suggesting the presence of biases between Tempel 1's center of brightness and center of mass. We rejected estimating these ever-changing biases; instead, the opnav data were combined with the ground-based astrometry measurements (Fig. 11), which resulted in comet ephemeris solution delivery K052/32 (Tables 7 and 8). TCM-3B was designed using this ephemeris, which required a constraint-free ΔV of 6 m/s to provide a Tempel 1 intercept trajectory at 05:52 ERT.

Once again, maneuver performance was excellent (Table 12). Postmaneuver orbit determination using only radiometric data estimated the target miss to be less than 1 km relative to design ephemeris K052/32 (Fig. 12). This targeting error was smaller than the 5-km go/no-go criteria summarized in Table 3, suggesting that TCM-5 might not be necessary. However, the flight system was still

Table 11 TCM-2 biasing strategy to improve TCM-1 telecom geometry [12]

	TCM-1 ΔV on 11 February 2005, 19:00 UTC							
TCM-2 ΔV, m/s	ΔV, m/s	RA,[a] deg	DEC,[a] deg	LGA-2, deg	Power, deg	ITS, deg	ΔV_{total}, m/s	$\Delta V_{\text{penalty}}$, m/s
0	27.7	175.1	−8.5	76.8	55.4	34.6	27.7	0
1	27.8	175.7	−6.6	75.4	56.1	33.9	28.8	1.2
2	28.1	176.2	−4.8	74.1	56.6	32.4	30.1	2.4
3	28.3	176.8	−3.0	73.1	57.1	32.9	31.3	3.6
4	28.6	177.4	−1.3	72.2	57.5	32.5	32.6	4.9

[a]Right ascension (RA) and declination (DEC) in EME2000.

Table 12 Design vs achieved TCM performance [12]

	Design			Achieved		
Maneuver	ΔV, m/s	RA,[a] deg	DEC,[a] deg	ΔV, m/s	RA,[a] deg	DEC,[a] deg
TCM-1	28.568	117.380	−1.280	28.561	117.390	−1.310
TCM-3A	5.045	21.00	−38.385	5.043	20.923	−38.385
TCM-3B	5.997	22.263	−24.721	5.997	22.263	−24.721
TCM-5.1	0.31	110.60	1.76	0.31	110.60	1.76
Divert	102.50	23.92	−27.43	102.50	23.92	−27.43

[a]Right ascension (RA) and declination (DEC) in EME2000.

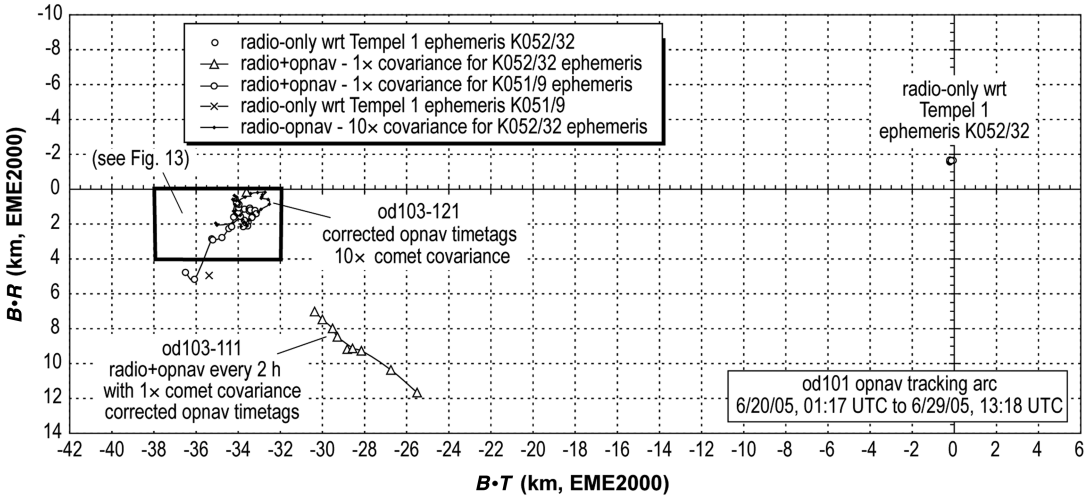

Fig. 12 Tempel 1 *B*-plane intercept estimates before TCM-5 at E − 30 h.

nearly 10 million kilometers from Tempel 1, too far away to draw this conclusion. We needed to acquire additional opnav much closer to the comet to more confidently determine the comet-relative trajectory before informed decisions about the need for TCM-5 could be made.

Encounter Phase

Beginning about 10 days before encounter, our analysis of opnav images began to distinguish the nucleus from the surrounding coma [11]. We first noticed this separation of nucleus and coma in the opnav residuals: the coma-induced biases tapered off, and a rotational signature became apparent. The photometric effects of the nucleus became evident several days later.

Orbit determination using both radiometric and optical data began estimating the flight system trajectory relative to Tempel 1. We began round-the-clock opnav image processing and orbit determination at E − 7 days when continuous comet imaging without flight system thermal constraints became possible (SPC < 120 deg). We performed orbit determination every 2 h using an ever-increasing opnav tracking arc so that we could closely monitor the *B*-plane intercept history in preparation for TCM-5 at E − 30 h [10]. Prelaunch analyses and encounter ORTs using simulated opnav images of Tempel 1 indicated that the long-arc solutions could describe a periodic "walk" in the *B*-plane, the presumed result of changing jet activity and shadowing effects as the nucleus rotates. For comparison, we computed short-arc orbit solutions based on the most recent opnav data covering a single rotation period, then estimated to be 42 h. These short-arc solutions could minimize the effect of rotational biases, because no part of the light curve would be sampled twice. The science team later estimated the comet rotation period to be 40.85 h [21].

TCM-5 was designed to correct only the *B*-plane target error [12], because the TOI errors were not observable in the opnav images. The most recent comet ephemeris was K052/7, which had a 1σ down-track ephemeris position uncertainty of 419 km, equivalent to a TOI uncertainty of 41 s (Table 7). These data led to the project decision to develop and validate the onboard encounter sequences assuming a ±3-min window centered on the chosen TOI target of 4 July 2005, 05:52 ERT. This conservative window size served as an acceptable upper bound on the TOI uncertainty, because ephemeris K052/7 was known to include systematic measurement errors [17]. When we excluded these ground-based observations from the data fit and added the most recent opnav data, the ephemeris 1σ down-track position uncertainty decreased to 180 km (K052/32). The 1σ TOI uncertainty reduced to ±17 s, well within the ±3-min window established to support onboard sequence development.

TCM-5 was to be executed only if the measured *B*-plane targeting error exceeded 5 km (Table 3). Orbit determination for the TCM-5.1 design, using opnav data up to 58 h before the maneuver at E − 30 h, indicated that the *B*-plane intercept was offset 34 km from the impact target, almost entirely in the $B \cdot T$ direction (Fig. 12). Correcting this comet-relative targeting error required a lateral ΔV of 31 cm/s (Table 12). Orbit determination using additional opnav data up to 10 h before TCM-5 would determine if we needed to implement the scheduled TCM-5.2 design update (Fig. 7).

Three comet-relative orbit determination strategies were initiated in preparation for the TCM-5.1 design. These solutions weighted the a priori comet ephemeris covariance for delivery K052/32 at 1×, 5×, and 10× to observe the effect on estimates of the comet ephemeris. Figure 13 compares the resulting periodic clockwise *B*-plane walk for the three cases. As the distance to Tempel 1 decreased, the three weighting strategies agreed better and better, always remaining confined to the same 4 × 4 comet-centered *B*-plane intercept space. By the time solution od164 was generated for the TCM-5.2 design, the *B*-plane intercepts for the three cases differed by less than 1 km. This superb consistency greatly increased our confidence in the baseline strategy (1× covariance weighting), as appropriate for the TCM-5 design.

Another measure of orbit solution consistency is evident in the Fig. 14 comparison between the baseline long-arc and the moving 42-h short-arc strategies. The long-arc results include labels for solutions od141 (5.1 design), and od164 (5.2 design). The *B*-plane intercepts for these two solutions were offset by just 700 m and provided essentially the same TOI estimate (Table 12). The good agreement between these two solutions, shown in Table 13, allowed the TCM-5.1 design to be implemented.

Once again, the flight system delivered excellent maneuver performance, because the ΔV parameters achieved by TCM-5 were not measurably different from the design values (Table 12). Figure 15 chronicles estimates of the *B*-plane coordinates achieved by TCM-5 relative to comet ephemeris K051/9. The first two estimates were limited to short arcs of postmaneuver radiometric data; the target miss distance was about 1.5 km with respect to K051/9. When postmaneuver opnav data were added and the comet ephemeris was estimated, the *B*-plane intercept shifted about 1 km toward the target. The good agreement between the radio-only and radio-with-opnav solutions suggested that the estimated ephemeris and K051/9 used to target TCM-5 were very similar, albeit based on a limited amount of postmaneuver opnav.

Two important decisions were made during the mission that added needed clarity to our navigation processes during the encounter phase. The first decision was to set aside the customary use of formal statistics provided by our orbit determination software as the primary basis for decision-making for TCM design and implementation. Instead, the best-estimate solutions themselves were directly compared with clearly specified go/no-go criteria (Table 3). The second decision, to generate orbit solutions covering perceived extremes in comet ephemeris covariance weighting, served to clearly validate the baseline strategy. Although the decision to compute orbit

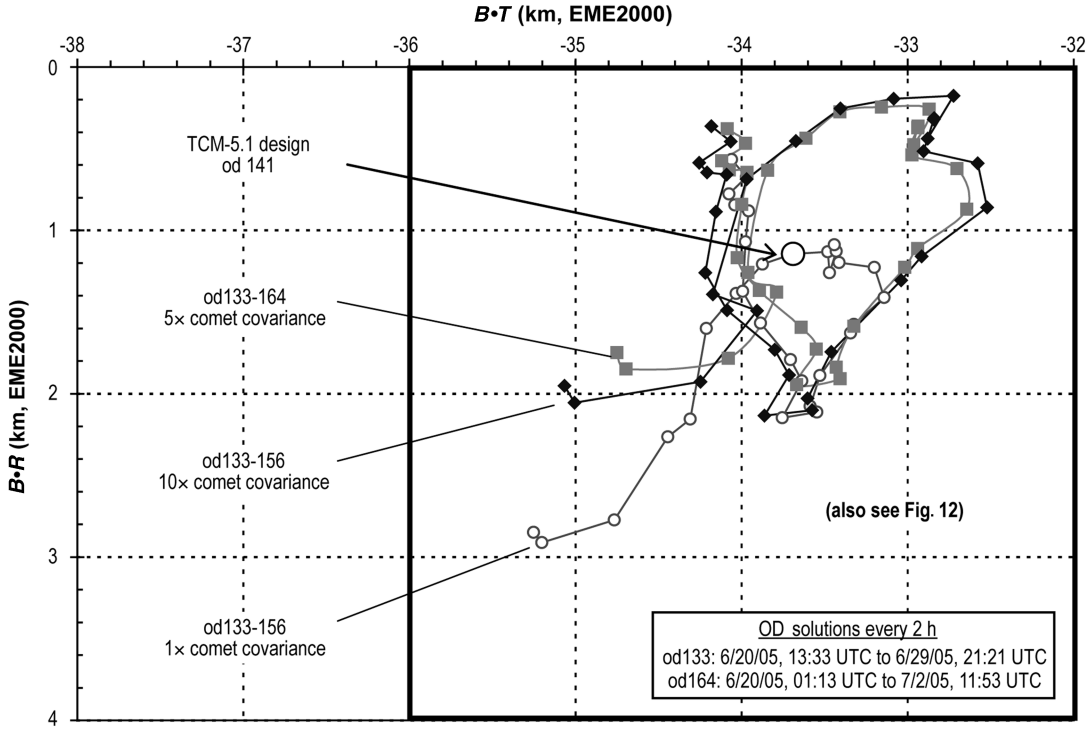

Fig. 13 ***B*-plane intercept comparisons of long-arc solutions using a priori Tempel 1 ephemeris covariance weightings of 1×, 5×, and 10× for K053/32 [10].**

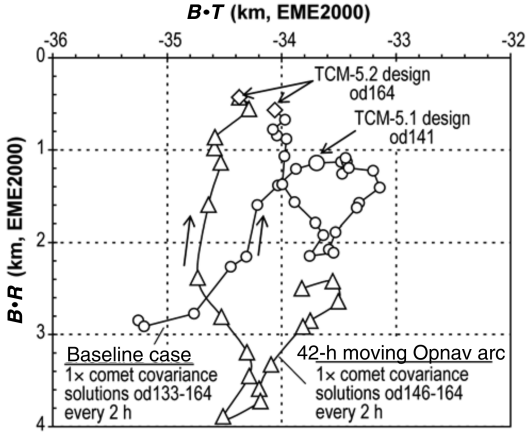

Fig. 14 ***B*-plane intercept history for the baseline orbit determination strategy (uses 1× the weighting of the a prior comet ephemeris covariance [10]).**

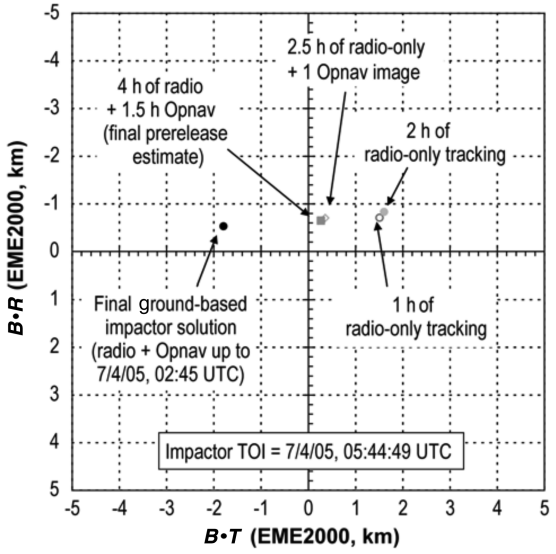

Fig. 15 ***B*-plane conditions achieved after impactor release [10].**

solutions every 2 h over the final week required a very demanding staffing effort, it paid off by clearly demonstrating a sustained pattern of solution consistency. The main objective became observing consistency between well-thought-out candidate strategies, while not getting too caught up in the formal statistics.

Impactor Release and the Flyby Divert

The impactor was released on schedule at E − 24 h and was positively identified soon afterward in an MRI image taken by the flyby. About 16 min after separation, the impactor autonomously computed and performed a detumble maneuver to regain attitude control by removing separation rates measured by onboard accelerometers. This 17-cm/s maneuver moved the impactor about 900 m further from a comet nucleus intercept. The impactor Autonav system then remained inactive until 2 h before impact in preparation for autonomous trajectory estimation and computation of three scheduled ITMs designed to result in impact in a sunlit area visible from the flyby (Fig. 4) [13,22].

Table 13 Comet-relative orbit solutions for TCM-5.1 and TCM-5.2 designs [10]

			Comet-relative orbit solutions (EME2000)			
Solution	Purpose	Opnav data cutoff (UTC)	$B \cdot R$, km	$B \cdot T$, km	B magnitude, km	Time of impact (UTC)
od141	TCM-5.1 design	29 June 2005, 22:00	0.25	−33.16	33.16	4 July 2005, 05:44:49.2
od164	TCM-5.2 design	2 July 2005, 13:00	0.38	−34.09	34.09	4 July 2005, 05:44:49.1

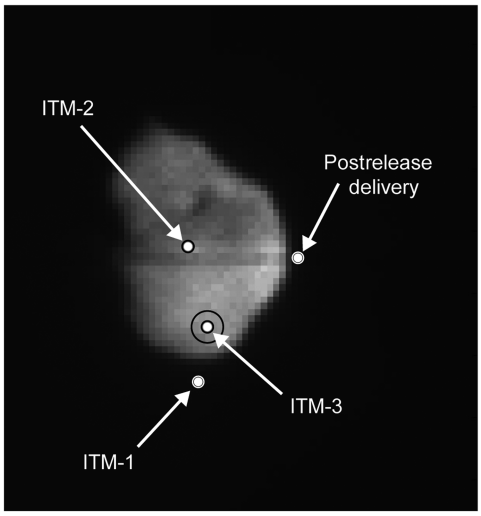

Fig. 16 Target intercepts achieved by three impactor ITMs (ITS image taken at E − 35 min [22]).

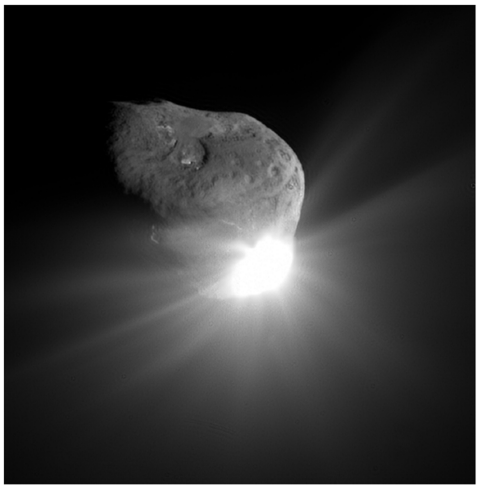

Fig. 17 Impactor collision with Tempel 1 as viewed by the flyby 67 s after impact (HRI deconvoluted image).

Twelve minutes after impactor separation, the flyby executed a divert maneuver of 102.5 m/s designed to achieve a flyby altitude of 500 km and to delay Tempel 1 closest approach by 850 s relative to *actual* impact. Postdivert orbit determination [10] based on radiometric data indicated that the flyby altitude was achieved within 3 km relative to Tempel 1 ephemeris solution K051/9, well within the 3σ control requirement of ± 50 km (Fig. 6). The desired flyby delay time was matched within 2 s, compared with the required 3σ control of ± 20 s. This impressive maneuver performance (Table 12) eliminated the need for the contingency divert trim maneuver scheduled at E − 12 h (Table 3).

Autonav Targeting

The impactor comet-relative trajectory was first determined by ground-based OD using opnav images acquired by the ITS, relayed to the flyby via an *S*-band link, and then downlinked. These orbit solutions served only to verify that the impactor was on the expected intercept trajectory. The flight system acquired all tracking data before impactor release; only opnav from the impactor's ITS were available after release. Figure 15 shows that the *B*-plane intercept for the final ground-based orbit solution had shifted about 2 km since the final prerelease orbit determination. The estimated TOI was 4 July 2005, 05:52:15 ERT, with a 1σ uncertainty of 11 s. This ground-based TOI estimate was 13 s later than the eventual impactor Autonav estimate and confirmed by images of the impact event taken every 0.2 s by the flyby.

At E − 2 h, identical Autonav systems onboard each spacecraft took control using autonomous target-tracking techniques for small bodies first developed by Bhaskaran et al. [23,24] for Stardust and Deep Space 1. The impactor Autonav system designed and executed three maneuvers, guiding the impactor into a path toward the sunlit limb of the comet. Meanwhile, Autonav onboard the flyby independently calculated the impactor trajectory and executed a series of slews to aim its instruments at the expected impact point, to turn the spacecraft to a shielded attitude as it flew past the comet, and to perform look-back imaging following the flyby (Fig. 4).

The impactor corrected only lateral trajectory errors determined using opnav images acquired by the ITS. The first ITM, at E − 90 min, was 1.27 m/s. Figure 16 shows that ITM-1 actually increased the nucleus miss distance to 7 km. Robust simulations of the attitude and gyro bias estimator had displayed this same behavior [25]. The encounter geometry and timing placed stringent limits on attitude-bias magnitude and drift, calling for sequenced tuning of the respective filters. An impactor attitude bias would be falsely interpreted by Autonav as a trajectory targeting error that would result in a maneuver computation error. At E − 90 min, the impactor was 55,600 km from Tempel 1. Based on impactor ground-based orbit determination at E − 3 h, the target miss was 1.8 km, correctable with an ITM-1 of 37 cm/s. A plausible attitude bias of 1 mrad could explain the Autonav computation of 1.27 m/s that moved the trajectory further off the comet nucleus, rather than closer.

At E − 35 min, the impactor performed ITM-2 when the range to Tempel 1 was 21,600 km. A lateral ΔV of 2.26 m/s computed and executed by the impactor moved the trajectory back onto the comet nucleus, once again using the center-of-brightness targeting technique. This maneuver resulted in a lateral trajectory change of 4.6 km and put the trajectory on an impact course, as shown in Fig. 16.

Before ITM-3, the image processing algorithm switched to scene analysis [13,22] to locate the preferred sunlit impact location. At a range of 7700 km, ITM-3 added a lateral trajectory change of 1.7 km with a ΔV of 2.28 m/s. This final trajectory adjustment was soon followed by the spectacular collision on 4 July 2005, 05:52:02 ERT, just 2 s later than the target TOI.

Figure 17 shows an HRI image of Tempel 1 taken 67 s after impact, from a distance of 79,900 km, at a pixel scale of 16 m/pixel [13]. This image was processed by experts at the Space Telescope Science Institute using deconvolution software algorithms to restore most of the resolution lost by the HRI focus problem.

Conclusions

Deep Impact's accomplishments were unprecedented and truly spectacular, but they did not come easily. There were many technical problems that threatened the schedule: an early mission descope with a smaller launch vehicle, a one-year launch delay, and many redesigns, some after launch. Important encounter ORTs could not be conducted for the first time until well after launch and some were based on new designs conceived after launch. Many activities had to be packed into a mission that lasted just 173 days. But the relentless efforts of a dedicated and talented flight team led to a smashing success. The flight system release of the impactor to within an estimated 2 km of an impact trajectory was a remarkable ground navigation achievement, and perhaps it made the impactor's incredibly clever job a little easier.

Along the way, there were several lessons learned that deserve mention:

Configuring safe mode at launch with coherency disabled put at risk timely acquisition by the second tracking pass (Madrid), because one-way Doppler and angles alone in the presence of a 1.6σ C_3 injection error were unable to determine the trajectory well enough to confidently update antenna-pointing predictions. A better balance of navigation and spacecraft risks would have coherency enabled during safe mode at launch. Once the injection orbit is confidently established after the start of the second tracking pass, the safe mode can be restored to coherency disabled without comprising navigation performance.

In-flight updates to the encounter timeline and the associated go/no-go criteria for critical events greatly simplified maneuver implementation decisions. Although these changes were beneficial across the entire flight team, they should have been defined, tested, and verified before launch.

Reliance on formal orbit determination statistics to make key navigation decisions proved to be an inappropriate strategy for this comet mission because of unknown biases between the center of brightness and the center of mass; scaling the comet ephemeris covariance to validate the baseline strategy was an excellent alternative. Future comet-bound navigators should strongly consider this strategy.

The use of ΔDOR proved to be a valuable measurement that helped achieve the solid radio-only heliocentric trajectory needed when adding opnav in the ground-based comet ephemeris improvement process. This measurement is valuable for any comet mission with demanding target delivery accuracy requirements.

TCM pointing constraints should be identified and reflected in the mission operations plan well before launch to assure adequate fuel margins, to establish appropriate maneuver design tools, procedures, and the attendant operational staffing levels. These constraints should be specified in requirement documents and audited for compliance.

The suite of opnav data reduction strategies, first introduced for Stardust, provided a consistent method of best locating the center of brightness in each opnav image. This very sound practice should continue.

Computing comet-relative orbit solutions every 2 h during the final week allowed close monitoring of the B-plane walk, leading to confident orbit determination and precise final targeting. This practice should be continued when precise targeting accuracy is required.

Acknowledgments

The research described in this paper was carried out at the Jet Propulsion Laboratory (JPL), California Institute of Technology under a contract with NASA. The authors, all members of the Deep Impact navigation team, are thankful for the support and guidance they received from several sources. Bill Blume, the Mission Design Manager, ably steered us through many updates to the mission design and helped prepare us for success. The JPL Guidance, Navigation, and Control Section leadership of Earl Maize and Al Cangahuala provided needed navigation resources and guided beneficial and timely peer reviews. The Navigation Advisory Group (NAG), created following the 1998 and 1999 Mars failures, continues to pay dividends through regular reviews of navigation plans and procedures for critical mission events. Key NAG contributors toward Deep Impact's navigation successes include Tim McElrath for his leadership in helping refine orbit determination strategies, Chris Potts for his thoughtful maneuver design suggestions, Steve Synnott for his considerable Opnav experience and leadership, and Shyam Bhaskaran for his Opnav operations guidance and experience. Shyam Bhaskaran also provided realistic simulated opnav images that helped make our encounter operational-readiness tests (ORTs) much more meaningful. A special thanks to John Michel and Francis Stienon for their very clever work to develop algorithms and implement software needed to quickly understand and satisfy our maneuver pointing constraints. The Deep Impact navigators also benefited from the influences of the Deep Impact red team led by "Renaissance man" Gentry Lee. Always the teacher, Gentry challenged us to treat our orbit determination statistics more thoughtfully: no more "BS covariance." Dave Spencer, the Deep Impact Mission Manager, skillfully guided the flight team through one unexpected challenge after another; Dave was also primarily responsible for valuable in-flight simplifications to the encounter timeline and trajectory correction maneuver go/no-go criteria. And, most important of all, a warm thanks to the families of all navigation team members who supported us throughout our amazing adventure.

References

[1] Kennedy, B. M., Riedel, J. E., Bhaskaran, S., Desai, S., Han, D., McElrath, T., Null, G., Ryne, M., Synnott, S., Wang, T.-C. M., and Werner, R., "Deep Space 1 Navigation: Primary Mission," *Deep Space Communications and Navigation Systems*, DESCANSO Design & Performance Summary Series, Jet Propulsion Lab., Pasadena, CA, Apr. 2004, http://descanso.jpl.nasa.gov/DPSummary/summary.cfm?force_external=0 [retrieved 23 Oct. 2007].

[2] Kennedy, B. M., Bhaskaran, S., Riedel, J. E., and Wang, T-C. M., "Deep Space 1 Navigation: Extended Missions," *Deep Space Communications and Navigation Systems*, DESCANSO Design & Performance Summary Series, Jet Propulsion Lab., Pasadena, CA, Sept. 2003, http://descanso.jpl.nasa.gov/DPSummary/summary.cfm?force_external=0 [retrieved 23 Oct. 2007].

[3] Carranza, E., Kennedy, B. M., and Williams, K. E., "Orbit Determination of Stardust from the Annefrank Asteroid Fly-By through the Wild 2 Comet Encounter," *AAS/AIAA Space Flight Mechanics Meeting*, Advances in the Astronautical Sciences, Vol. 119, Part 2, American Astronautical Society, San Diego, CA, 2005, pp. 1861–1879.

[4] Bhat, R. S., Williams, K. E., Helfrich, C. E., Kennedy, B. M., and Carranza, E., "Wild 2 Approach Maneuver Strategy Used for Stardust Spacecraft," *Proceedings of the AIAA/AAS Astrodynamics Specialist Conference*, American Astronautical Society, San Diego, CA, Aug. 2004, pp. 1–20.

[5] Bhaskaran, S., Mastrodemos, N., Riedel, J. E., and Synnott, S. P., "Optical Navigation for the Stardust Wild 2 Encounter," *Proceedings of the 18th International Symposium on Space Flight Dynamics*, American Astronautical Society, San Diego, CA, Oct. 2004, p. 455.

[6] Blume, W. H., "Deep Impact: Mission Design Approach for a New Discovery Mission," *Acta Astronautica*, Vol. 52, Nos. 2–6, Jan. 2003, pp. 105–110. doi:10.1016/S0094-5765(02)00144-3

[7] A'Hearn, M., Delamere, A., and Frazier, W., "The Deep Impact Mission: Opening a New Chapter in Cometary Science," International Astronautical Congress Paper 00-IAA.11.2.04, Oct. 2000.

[8] A'Hearn, M. F., Belton, M. J. S., Delamere, W. A., Kissel, J., Klaasen, K. P., McFadden, L. A., et al., "Deep Impact: Excavating Comet Tempel 1," *Science*, Vol. 310, No. 5746, 2005, pp. 258–264. doi:10.1126/science.1118923

[9] Blume, W. H., "Deep Impact Mission Design," *Space Science Reviews*, Vol. 117, Nos. 1–2, Mar. 2005, pp. 23–42. doi:10.1007/s11214-005-3386-4

[10] Ryne, M., Jefferson, D., Craig, D., Higa, E., Lewis, G., and Menon, P., "Ground-Based Orbit Determination for Deep Impact," *16th Annual AAS/AIAA Space Flight Mechanics Meeting*, American Astronautical Society, San Diego, CA, Jan. 2006, pp. 1179–1202.

[11] Owen, W. M., Jr., Mastrodemos, N., Rush, B. P., Wang, T.-C. M., Gillam, S. D., and Bhaskaran, S., "Optical Navigation for Deep Impact," *16th Annual AAS/AIAA Space Flight Mechanics Meeting*, American Astronautical Society, San Diego, CA, Jan. 2006, pp. 1231–1250.

[12] Bhat, R. S., Stumpf, P. W., and Frauenholz, R. B., "Deep Impact Ground Navigation Maneuver Design and Performance," *16th Annual AAS/AIAA Space Flight Mechanics Meeting*, American Astronautical Society, San Diego, CA, Jan. 2006, pp. 1203–1230.

[13] Mastrodemos, N., Kubitschek, D. G., Werner, R. A., Kennedy, B. M., Synnott, S. P., Riedel, J. E., Bhaskaran, S., Null, G. W., and Vaughan, A. T., "Autonomous Navigation for Deep Impact," *16th Annual AAS/AIAA Space Flight Mechanics Meeting*, American Astronautical Society, San Diego, CA, Jan. 2006, pp. 1251–1270.

[14] Muench, R. E., Sagdeev, R. Z., and Jordan, J. F., "Pathfinder: Accuracy Improvement of Comet Halley Trajectory for Giotto Navigation," *Nature*, Vol. 321, May 1986, pp. 318–320. doi:10.1038/321318a0

[15] Yeomans, D. K., Giorgini, J. D., and Chesley, S. R., "The History and Dynamics of Comet 9P/Tempel 1," *Space Science Reviews*, Vol. 117, Nos. 1–2, Mar. 2005, pp. 123–135. doi:10.1007/s11214-005-3392-6

[16] Marsden, B. G., "On the Orbits of Some Long-Lost Comets," *The Astronomical Journal*, Vol. 68, No. 10, Dec. 1963, pp. 795–801. doi:10.1086/109217

[17] Chesley, S. R., and Yeomans, D. K., "Comet 9P/Tempel 1 Ephemeris Development for the Deep Impact Mission," *16th Annual AAS/AIAA Space Flight Mechanics Meeting*, American Astronautical Society, San Diego, CA, Jan. 2006, pp. 1271–1282.

[18] Meech, K. J., Ageorges, N., A'Hearn, M. F., Arpigny, C., Ates, A., Aycock, J., et al., "The Deep Impact Earth-Based Campaign," *Space*

Science Reviews, Vol. 117, Mar. 2005, pp. 297–334.
doi:10.1007/s11214-005-3382-8

[19] Meech, K. J., Ageorges, N., A'Hearn, M. F., Arpigny, C., Ates, A., Aycock, J., et al., "Deep Impact: Observations from a Worldwide Earth-Based Campaign," *Science*, Vol. 310, No. 5746, Oct. 2005, pp. 265–269.
doi:10.1126/science.1118978

[20] Marsden, B. G., Sekanina, Z., and Yeomans, D., "Comets and Nongravitational Forces," *Astronomical Journal*, Vol. 78, No. 2, Mar. 1973, pp. 211–225.
doi:10.1086/111402

[21] Belton, M. J. S., Meech, K. J., A'Hearn, M. F., Groussin, O., McFadden, L., Lisse, C., et al., "Deep Impact: Working Properties for the Target Nucleus–comet 9P/Tempel 1," *Space Science Reviews*, Vol. 117, Mar. 2005, pp. 137–160.
doi:10.1007/s11214-005-3389-1

[22] Kubitschek, D. G., Mastrodemos, N., Werner, R. A., Kennedy, B. M., Synnott, S. P., Null, G. W., Bhaskaran, S., Riedel, J. E., and Vaughan, A. T., "Deep Impact Autonomous Navigation: The Trials of Targeting the Unknown," *29th Annual AAS Rocky Mountain Guidance and Control Conference*, American Astronautical Society, San Diego, CA, Feb. 2006, pp. 381–406.

[23] Bhaskaran, S., Riedel, J. E., and Synnott, S. P., "Autonomous Nucleus Tracking for Comet/Asteroid Encounters: The STARDUST Example," *Proceedings of the 1998 IEEE Aerospace Conference*, Vol. 1, Inst. of Electrical and Electronics Engineers, Piscataway, NJ, 1998, pp. 353–365.

[24] Bhaskaran, S., Riedel, J. E., and Synnott, S. P., "Autonomous Target Tracking for Small Bodies During Flybys," *14th Annual AAS/AIAA Space Flight Mechanics Meeting*, American Astronautical Society, San Diego, CA, Feb. 2004, pp. 2079–2096.

[25] Hughes, M. P., Schira, C., and Kendall, L., "Deep Impact Attitude Estimator Design and Flight Performance," *29th Annual AAS Rocky Mountain Guidance and Control Conference*, American Astronautical Society, San Diego, CA, Feb. 2006, pp. 441–468.

C. McLaughlin
Associate Editor